

EPLAB

THE EPPLEY LABORATORY, INC.

SCIENTIFIC INSTRUMENTS

NEWPORT, R.I.

U.S.A.

N65-19883

FACILITY FORM 502

(ACCESSION NUMBER)	(THRU)
72	1
(PAGES)	(CODE)
CR-57509	14
(NASA CR OR TMX OR AD NUMBER)	(CATEGORY)

FINAL TECHNICAL REPORT

DESIGN STUDY

SOLAR SPECTRAL MEASUREMENT PROGRAM

(JPL CONTRACT NO. 950929)

Prepared for

The Jet Propulsion Laboratory,
4800 Oak Grove Drive,
Pasadena, California.

GPO PRICE \$ _____

OTS PRICE(S) \$ _____

Hard copy (HC)

\$3.00

Microfiche (MF)

\$0.75

1 August 1964

EPLAB

THE EPPLEY LABORATORY, INC.
SCIENTIFIC INSTRUMENTS
NEWPORT, R.I.
U.S.A.

FINAL TECHNICAL REPORT
DESIGN STUDY
SOLAR SPECTRAL MEASUREMENT PROGRAM
(JPL CONTRACT NO. 950929)

This work was performed for the Jet Propulsion Laboratory,
California Institute of Technology, sponsored by the
National Aeronautics and Space Administration under
Contract NAS7-100.

Prepared for
The Jet Propulsion Laboratory,
4800 Oak Grove Drive,
Pasadena, California.

1 August 1964

FINAL TECHNICAL REPORT

JET PROPULSION LABORATORY CONTRACT NO. 950929

DESIGN STUDY

SOLAR SPECTRAL MEASUREMENT PROGRAM

A. J. Drummond
Project Director

1 August 1964

TABLE OF CONTENTS

	Page
LIST OF FIGURES	iv
LIST OF TABLES	vii
1. INTRODUCTION	1
2. DETECTOR DEVELOPMENT AND TEST PROGRAMS	3
2.1 General	3
2.2 Specific requirements for the JPL-Eppley project	4
2.3 Development and fabrication of fast-response thermopiles	6
2.4 Determination of performance characteristics of the new thermopile prototypes in air and in vacuum	10
2.4.1 Time response	11
2.4.2 Sensitivity, Linearity and Repeatability	11
2.4.3 Temperature dependence of sensitivity	11
2.4.4 Temperature compensation of sensitivity	12
2.4.5 Wavelength sensitivity	16
2.5 Shock tests	16
2.5.1 Mechanical	17
2.5.2 Thermal	17
3. FILTER RADIOMETRY	17
3.1 General	17
3.2 Specific requirements for the JPL-Eppley project	19
3.3 Filter development	19
3.4.1 Spectral transmittance with special reference to primary and secondary bandpass characteristics	21
3.4.2 Spectral transmittance with special reference to angle of incidence of irradiation	21

TABLE OF CONTENTS (Cont.)

	Page
3.5 Shock tests	21
3.5.1 Mechanical (air-vacuum)	21
3.5.2 Solarization (UV radiation)	21
4. DETECTOR SIGNAL OPTICAL AMPLIFICATION	22
4.1 Choice of lens	22
4.2 Lens tests	23
5. CALIBRATION PROCEDURES FOR DETECTOR SYSTEMS	25
5.1 In sunlight	25
5.2 In the laboratory	25
6. DETERMINATION OF DETECTOR (HEAT SINK) TEMPERATURE	27
7. ACKNOWLEDGEMENTS	28
8. REFERENCES	29

LIST OF FIGURES

	Page
Fig. 1 Technique adopted to clean the anodized aluminum thermopile body (electro-chemical process)	8.a
Fig. 2 Apparatus for winding the new type thermopile element	8.b
Fig. 3 Apparatus for electro-plating the new type thermopiles	8.c
Fig. 4 Diagram of the wire winding apparatus	8.d
Fig. 5 Diagram of the electro-plating bath	8.e
Fig. 6 Schematic diagram of the electrical circuit employed in the control unit of the cleaning apparatus	8.f
Fig. 7 Schematic diagram of the electrical circuit employed in the control unit of the electro-plating apparatus	8.g
Fig. 8 Diagram showing the construction principle of the new fast-response type of Eppley thermopile (prototype models I and II)	10.a
Fig. 9 Diagram showing the construction principle of the new fast-response type of Eppley thermopile (prototype model III)	10.b
Fig. 10 Illustration of the time response of the new Eppley thermopile models (i.e. $<10^{-4}$ torr), using an oscilloscope with camera attachment	11.b
Fig. 11 Sensitivity of the new Eppley thermopile models, in air and in vacuum (i.e. $<10^{-4}$ torr), as a function of radiant flux density - 50 to 200 mw cm ⁻²	11.c
Fig. 12 Temperature dependence of sensitivity of the new Eppley thermopile models in air - ambient temperature range -70 to +90° C	11.d

LIST OF FIGURES (Cont.)

	Page
Fig. 13 Temperature dependence of sensitivity of the new Eppley thermopile model III in vacuum (i.e. $<10^{-4}$ torr) - ambient temperature range 0 to $+70^{\circ}$ C	11.e
Fig. 14 Spectral transmittance of a typical narrow bandpass (i.e. interference type) filter in the middle UV region for (a) normal incidence radiation and (b) when tilted 5 and 10° to normal - actual scale	21.a
Fig. 15 Spectral transmittance of a typical narrow bandpass (i.e. interference type) filter in the middle UV region - expanded ordinate scale	21.b
Fig. 16 Spectral transmittance of a second typical (broader limits) narrow bandpass filter in the middle UV region - expanded ordinate scale	21.c
Fig. 17 Spectral transmittance of a third typical narrow bandpass filter in the near UV region - expanded ordinate scale	21.d
Fig. 18 Secondary transmittance of 7 typical UV narrow bandpass filters (including the 3 filters of Figs. 14-17) in the visible region: primary bandpasses 250-300, 275-300, 300-325 and 300-350 $m\mu$ - ordinate scale expanded $\approx \times 10$	21.e
Fig. 19 Secondary transmittance of 7 typical UV narrow bandpass filters (including the 3 filters of Figs. 14-17) in the near IR region: primary bandpasses 250-300, 275-300, 300-325 and 300-350 $m\mu$ - ordinate scale expanded $\approx \times 10$	21.f

LIST OF FIGURES (Cont.)

	Page
Fig. 20 Spectral transmittance of a typical narrow band-pass filter in the visible region - actual scale	21.g
Fig. 21 Spectral transmittance of a second typical narrow bandpass filter in the near IR region - actual scale	21.h
Fig. 22 Spectral transmittance of a first series of 4 UV narrow bandpass filters before exposure, in a vacuum system, to UV radiation - actual scale	21.j
Fig. 23 Spectral transmittance of a first series of 4 UV narrow bandpass filters after exposure, in a vacuum system, to UV radiation - actual scale	21.k
Fig. 24 Spectral transmittance of a second series of 3 UV narrow bandpass filters before exposure, in a vacuum system, to UV radiation - actual scale	21.m
Fig. 25 Spectral transmittance of a second series of 3 UV narrow bandpass filters after exposure, in a vacuum system, to UV radiation - actual scale	21.n
Fig. 26 Examples of the dependence of the filter factor for narrow bandpass selectivity on source emission characteristics (solar optical air mass = 0, 1 and 5)	29.a
Fig. 27 The spectral distribution of the extraterrestrial solar radiation, according to (a) Johnson and (b) Nicolet	29.b

LIST OF TABLES

	Page
TABLE I The extraterrestrial radiation of the sun (Earth solar constant)	1.a,1.b
TABLE II Total daily radiation on a horizontal plane at the upper limit of the Earth's atmosphere: mean values for calendar months in $\text{cal cm}^{-2} \text{ day}^{-1}$ (solar constant value of $1.98 \text{ cal cm}^{-2} \text{ min}^{-1}$)	1.c
TABLE III Performance characteristics of the first proto- type models of the new fast-response type of Eppley thermopile	11.a
TABLE IV Response of the new Eppley thermopile with re- spect to the wavelength of the incident radiation	16.a
TABLE V Provisional selection of wavelength intervals (10) to be isolated by filters in the JPL-Eppley Solar Spectral Measurement Experiment	19.a
TABLE VI Examples of the mutual consistency of Eppley high-intensity thermopile calibrations: solar- laboratory transfer (air operation)	25.a,25.b

1. INTRODUCTION

The extraterrestrial flux of solar radiation, integrated over all emission wavelengths, is generally referred to as the Earth solar constant. It is the rate at which energy is received upon unit surface, perpendicular to the sun's beam, in free space at the Earth's mean distance from the sun. A precise knowledge of the energy in different regions of the extraterrestrial solar spectrum is important for handling many geophysical problems, such as those involved in determination of the thermal balance of the upper atmosphere and the related aspects of the radiative equilibrium of spacecraft.

During the last 25 years, estimates of the total solar irradiance at the outer limit of the terrestrial atmosphere have ranged from about 130 to 145 mw cm⁻². At present, the evaluations which have found most support are those of Johnson¹ (139.5 mw cm⁻²) and Nicolet^{2,3} (138 mw cm⁻²). For details, see Tables I and II and Fig. 27 of this Report. There is, however, an important point which must be borne in mind when considering these figures; whereas Johnson has assigned reliability limits of ± 2 per cent to his derived solar constant, Nicolet is much more conservative and argues that this uncertainty could be as great as ± 5 per cent. A further problem is imposed by the limitations of current knowledge of the basic radiation reference. While it is believed that the International Pyrheliometric Scale, introduced in 1956, represents the true radiative standard to within 0.5 per cent, it is possible that the uncertainty may be as great as 1 per cent. Practically all approaches to solar constant determination have involved, essentially, a study of the classical measurements made during the last half century by Abbot and his

TABLE I The Extraterrestrial Radiation of the Sun (Earth Solar Constant)

Percentage in spectral regions ($\Delta\lambda=0.01 \mu$) according to Johnson (J)*
and Nicolet (N)**

$\lambda(\mu)$	John- son	Nic- olet	Mean	$\frac{J-N}{J}\%$	(J-N)	$\lambda(\mu)$	John- son	Nic- olet	Mean	$\frac{J-N}{J}\%$	(J-N)
0.22	0.02	0.01	0.02	+50	+0.01	0.44	1.45	1.38	1.41	+5	+0.07
.23	.04	.03	.03	+25	+0.01	.45	.58	.52	.55	+4	+0.06
.24	.04	.03	.04	+25	+0.01	.46	.55	.56	.56	+1	+0.01
.25	.05	.04	.05	+20	+0.01	.47	.56	.57	.56	-1	-0.01
.26	.09	.10	.09	-10	-0.01	.48	.55	.57	.56	-1	-0.02
.27	.18	.12	.15	+34	+0.60	.49	.43	.46	.45	-2	-0.03
.28	.17	.11	.14	+35	+0.60	.50	.42	.50	.46	-5	-0.08
.29	.37	.26	.32	+30	+0.11	.51	.41	.50	.46	-6	-0.09
.30	.44	.30	.37	+32	+0.14	.52	.34	.40	.38	-4	-0.05
.31	.54	.45	.49	+17	+0.90	.53	.40	.46	.43	-4	-0.06
.32	.61	.52	.57	+15	+0.90	.54	.42	.46	.44	-3	-0.04
.33	.82	.64	.73	+22	+0.18	.55	.40	.39	.40	+1	+0.01
.34	.80	.63	.71	+21	+0.17	.56	.36	.45	.40	-7	-0.09
.35	.85	.66	.75	+22	+0.19	.57	.34	.43	.39	-7	-0.09
.36	.83	.68	.76	+20	+0.17	.58	.34	.43	.38	-7	-0.09
.37	.95	.68	.81	+18	+0.17	.59	.32	.38	.35	-5	-0.06
.38	.88	.67	.78	+22	+0.19	.60	.30	.37	.33	-5	-0.07
.39	0.80	0.72	0.76	+10	+0.08	.61	.27	.33	.30	-6	-0.06
.40	1.10	1.12	1.11	- 2	-0.02	.62	.25	.30	.28	-4	-0.05
.41	.39	.27	.33	+ 8	+0.12	.63	.22	.27	.24	-4	-0.05
.42	.38	.27	.32	+ 8	+0.11	.64	.19	.24	.21	-4	-0.05
0.43	1.28	1.19	1.24	+ 7	+0.09	0.65	1.16	1.21	1.19	-5	-0.05

* J. Meteor., 11, 431, 1954 ** Archiv. Meteor., Geoph., Biokl., A, 3,
209, 1951

1.b

$\lambda(\mu)$	John- son	Nic- olet	Mean	$\frac{J-N}{J}\%$	(J-N)	$\lambda(\mu)$	John- son	Nic- olet	Mean	$\frac{J-N}{J}\%$	(J-N)
0.66	1.14	1.19	1.17	- 4	-.05	1.80	0.11	0.12	0.11	- 9	-.01
.67	.11	.16	.14	- 4	-.05	1.90	.09	.10	.10	-10	-.01
.68	.08	.13	.11	- 4	-.04	2.00	.08	.08	.08	0	0
.69	.06	.11	.08	- 5	-.05	.10	.07	.07	.07	0	0
.70	.03	.07	.05	- 4	-.04	.20	.06	.06	.06	0	0
.71	1.01	.05	.03	- 4	-.04	.30	.05	.05	.05	0	0
.72	0.98	.02	1.00	- 2	-.02	.40	.04	.04	.04	0	0
.73	.96	1.00	0.98	- 4	-.01	.50	.04	.03	.04	0	0
.74	.93	0.96	.95	- 3	-.03	.60	.03	.03	.03	0	0
.75	.91	.94	.92	- 3	-.03	.70	.03	.03	.03	0	0
.80	.81	.83	.82	- 3	-.02	.80	.02	.02	.02	0	0
.85	.72	.75	.73	- 4	-.03	2.90	.02	.02	.02	0	0
.90	.64	.68	.66	- 4	-.04	3.00	.02	.02	.02	0	0
0.95	.58	.61	.60	- 5	-.03	.10	.02	.02	.02	0	0
1.00	.52	.55	.54	- 6	-.03	.20	.02	.02	.02	0	0
.10	.43	.44	.43	- 2	+.01	.30	.01	.01	.01	0	0
.20	.36	.36	.36	0	0	.40	.01	.01	.01	0	0
.30	.29	.31	.30	- 2	-.01	.50	.01	.01	.01	0	0
.40	.24	.26	.25	- 4	-.01	.60	.01	.01	.01	0	0
.50	.19	.22	.21	-15	-.03	.70	.01	.01	.01	0	0
.60	.16	.19	.17	-19	-.03	.80	.01	.01	.01	0	0
1.70	0.13	0.15	0.14	-15	-.02	3.90	0.01	0.01	0.01	0	0

SUMMARY Ultra-violet ($\lambda \leq 0.38\mu$) Visible ($\lambda 0.38-0.75\mu$)
 % 7.2(J) 5.6(N) 6.4(M) 46.4(J) 47.2(N) 46.8(M)

Infra-red ($\lambda > 0.75\mu$)
 % 46.4(J) 47.2(N) 46.8(M)

1.c

TABLE II Total Daily Radiation on a Horizontal Plane at the Upper Limit of the Earth's Atmosphere: Mean Values for Calendar Months in $\text{Cal Cm}^{-2} \text{ Day}^{-1}$ (Solar Constant Value of $1.98 \text{ Cal Cm}^{-2} \text{ Min}^{-1}$)

LATITUDE	60°N	50°N	40°N	30°N	20°N	10°N	0°	10°S	20°S	30°S	40°S
January	83	221	369	516	653	772	875	957	1010	1039	1039
February	211	354	495	626	740	836	906	951	964	954	916
March	413	549	667	764	840	890	914	909	875	816	734
April	661	759	831	889	915	915	884	831	753	651	531
May	881	926	960	967	949	907	838	750	642	515	378
June	988	1003	1007	993	955	893	809	706	583	451	309
July	941	968	986	977	949	896	819	722	608	478	341
August	762	829	886	918	925	904	858	793	699	585	460
September	520	635	733	814	868	895	896	871	818	741	642
October	283	426	558	676	776	852	902	928	924	895	833
November	122	261	408	552	680	791	879	948	991	1006	991
December	58	183	329	482	625	752	860	951	1016	1056	1073

2.

co-workers at the Astrophysical Observatory of the Smithsonian Institution in Washington. The divergence between the radiation reference adopted by Abbot (and also, inherently, by Johnson and Nicolet), viz. The Smithsonian Scale of 1913, and the International Pyrheliometric Scale is now set at 2.0 per cent, the latter being the lower.

It is therefore quite clear that any solar constant figure derived from treatment of the Smithsonian basic data assembled at high mountain sites (and supplemented mainly by rocket ascents undertaken by the U. S. Naval Research Laboratory) is uncertain by at least 5 per cent.

The continuous solar spectrum has not been observed beyond the limit of the terrestrial atmosphere and, as a result, there still remain very considerable discrepancies between the values reported by the various authors, particularly for wavelengths shorter than 500 mμ, although such divergence does extend through the visible into the near infra-red region.

The increasing complexity of artificial satellites and spacecraft, and in the case of the spacecraft, the change in solar exposure occasioned by such voyages as those towards Venus and Mars requires sophisticated thermal control systems. Equally important is the need for adequate ground test facilities. While there have been marked improvements in the stability, uniformity and efficiency of solar simulation systems, the problem of spectral distribution of energy still requires serious attention. Techniques of measurement, monitoring and modification of the spectrum of artificial sources today represent broad areas of increased activity, which if they are to

3.

be fully developed, must clearly be based upon an optimum knowledge of the sun's spectral radiance and also of the absolute irradiances of surfaces in spacial environment. There is no question that use of the D.C. thermopile represents the most practical approach to the absolute evaluation of radiometric flux, totally or spectrally employing filter isolating techniques. The present state of the art in precision radiometry is such as to encourage an effort to re-examine, experimentally, the integral wavelength extraterrestrial solar emission and its spectral energy distribution in, at least, certain wavebands of paramount interest in spacecraft operation. Such a potential examination is therefore the principal object of the Design Study reported upon here. It will be recognized that important contributing factors to the measurement (and resulting data interpretation) accuracy are the state of manufacture of filter optical configuration and the stability of filter transmission characteristics (as well as those of the basic detector when constructed for this usage) in free space operation.

2. DETECTOR DEVELOPMENT AND TEST PROGRAM

2.1 General

At present, thermal radiation detectors for use in upper atmospheric or space studies may be considered as falling generally into several classes, viz:

- (a) Thermopiles (true junctions);
- (b) Thermopiles (artificial junctions - either electrochemically or vacuum deposited);
- (c) Thermocouples (1 or few thermo-junctions) requiring optical

4.

amplification of detector signal;

(d) Thermistor bolometers.

Their performance characteristics, in each case, are not mutually independent. For instance, fast detector response may have to be achieved (as has generally been the case) at the expense of uniformity in the response with regard to the wavelength of the incident energy, on account of the necessity to employ very thin receiver blackenings.

When absolute measurements are desired, there is no question that the thermopile is the best detector. It is believed that a properly designed unit with thermo-elements prepared artificially by electro-plating should be very robust without impairing stability of performance over reasonable periods of time. Some experiments made at the Eppley Laboratory, prior to the commencement of work on the subject study contract, indicated that a time response of less than 1 second ($1/e$ signal in air) could be achieved with such an "artificial" thermopile, as well as sensitivity comparable to that of the classical soldered construction type.

2.2 Specific requirements for the JPL-Eppley project

These may be summarized as follows:

- (a) Good repeatability of detector signal (i.e. repetition of radiometer output with radiation intensity varying rapidly between zero and a chosen fixed value, to within ± 1 per cent);
- (b) Good stability of radiometer (i.e. detector, lens and filter system) performance over the period of operation, e.g. ± 1 per cent constancy for a continuous exposure time of at least 1 month under vacuum conditions;

5.

- (c) Detector time response faster than 3 seconds for 98 per cent signal (i.e. 0.75 second for $1/e$ signal) in vacuum;
- (d) Detector sensitivity to be optimum, commensurate with adherence to adequate time response (e.g. a figure of 5 mv per cal $\text{cm}^{-2} \text{min}^{-1}$ in vacuum is the initially Eppley proposed target);
- (e) Minimum dependence of detector response on ambient temperature and measurement of the latter value;
- (f) Uniformity of detector response over the wavelength range 0.25-2.5 μ , to facilitate instrument calibration and evaluation of measured data;
- (g) Adequate filter bandpass characteristics, i.e. for definition of wavelength interval isolated, for a detector signal capable of accurate measurement and for high certainty of interpretation of the filter measurement;
- (h) Meeting the amplifier-readout system requirement, viz. minimum signal for any radiometer channel exposure of 0.25 mv, with all amplifier etc. output signals to approach a maximum figure as nearly as possible of 4 v - this necessitates optical amplification of the detector, e.g. through use of a (quartz) lens;
- (i) Introduction of calibration procedures with the object of establishing detector system calibration (in the laboratory with the Johnson extraterrestrial solar curve as reference) with an accuracy of within ± 2 per cent, assuming that the International Pyrheliometric Scale is completely free from uncertainty;
- (j) Environmental survival (i.e. successful subjection to mechanical and thermal shocks as dictated by the JPL requirements in these respects);

6.

(k) Radiometer-amplifier etc. package dimensions and mass in accordance with the JPL requirements.

As detector, the electro-chemically formed artificial thermopile is proposed for this project. Experience at the Eppley Laboratory indicates that a true thermo-junction thermopile construction will not be sufficiently robust for the purpose if the time response and sensitivity requirements are to be met. The use of evaporated junctions at greatly reduced pressures (e.g. $<10^{-10}$ torr) does not inspire confidence on account of their general thinness, and therefore their tendency to rapidly re-evaporate, resulting in dangerously thin layers, in space exposure: the production of thick evaporated films has difficulties.

A new technique for the manufacture of electro-chemically coated detectors is described in the next section of this report: fast response together with good sensitivity were the objectives of this development project.

2.3 Development and fabrication of fast-response thermopiles

In the introduction of the new type of thermopile the following philosophy dictated the design: (a) a continuous fine wire construction without soldered joint interruptions; (b) the choice of constantan wire, on account of its relative constancy of electrical resistivity and its ductability over the great range of ambient temperature which may be encountered; (c) good adherence of a copper deposit to constantan over a wide temperature range; the use of copper as the second thermo-element reduces substantially the impedance of the thermopile; (d) the choice of anodized aluminum for the thermo-

7.

pile body combines good electrical insulation with adequate thermal conductivity (silver and copper are difficult to insulate electrically, commercially, through a chemical process), e.g. aluminum anodized to a thickness of 0.004 inch resists an imposed voltage of 300 v; (e) anodized aluminum resists weather corrosion effects.

The first three artificial thermopiles of the type described here (i.e. prototype models I-III) were constructed of normally available commercial aluminum. A feature of this design is the cutting of a number of grooves into the vertical cylindrical wall of the thermopile body in which to thread the constantan wire. Since these grooves are somewhat rough on account of the machining (milling) to separate grooves 0.004 to 0.008 inch apart, a very careful anodizing process is necessary to prevent the edges from rupturing (and thus destroying the electrical insulation). It has been found that a chemical cleaning procedure, prior to the anodizing stage, enables the latter operation to be effected with a much smoother surface result. Another important aspect of the anodizing technique is the obtaining of a continuous electrical insulated surface, i.e. the obviation of porous materials which cannot be properly insulated. This problem is further aggravated by the fact that the aforementioned cleaning process, to achieve a hard anodized coating, is one which utilizes organic solvents which, in turn, can penetrate such pores in the aluminum body and further induce electrical leakage. A special process is therefore necessary, after the basic anodizing, to seal these microscopic pores. With this object, the Adodite Company (recommended by JPL) has proposed the use of Alcoa 6061 aluminum.

8.

The terminals of the thermopile are copper. The soldering procedure is as recommended in the JPL specifications, thermal-free solder being employed. The screws securing the terminals and also to anchor the thermopile body to a main heat sink are produced from hard anodized (6061) aluminum. Because of the difficulty in anodizing tapped holes, the screws have to be insulated electrically with Teflon bushings before insertion. All four screws (i.e. 2 terminal and 2 body holders) are secured through a copper retaining washer to ensure rigidity.

Fig. 1 shows the electro-chemical cleaning process, Fig. 2 the wire winding apparatus, and Fig. 3 the electro-plating bath. Schematic diagrams of the wire winding and electro-plating equipment are given, respectively, in Figs. 4 and 5. A block diagram of the electrical circuit employed in the control unit of the cleaning apparatus is reproduced in Fig. 6, as is also a similar diagram of the control unit of the electro-plating apparatus in Fig. 7.

Winding such fine wires (e.g. 0.06 mm) is a rather difficult operation since the wire must not be contaminated by personal contact which would result in poor electro-plating. Hence, a special winding device had to be constructed for this purpose, where precise guiding of the wire over the thermopile body is achieved. In order to vary the separation distance of the windings (e.g. to produce different multi-junction thermopiles) the (interchangeable) gear system, shown in Fig. 2, was introduced. During this winding operation the wire is maintained under constant tension by a suitable weight suspended at the free extremity.

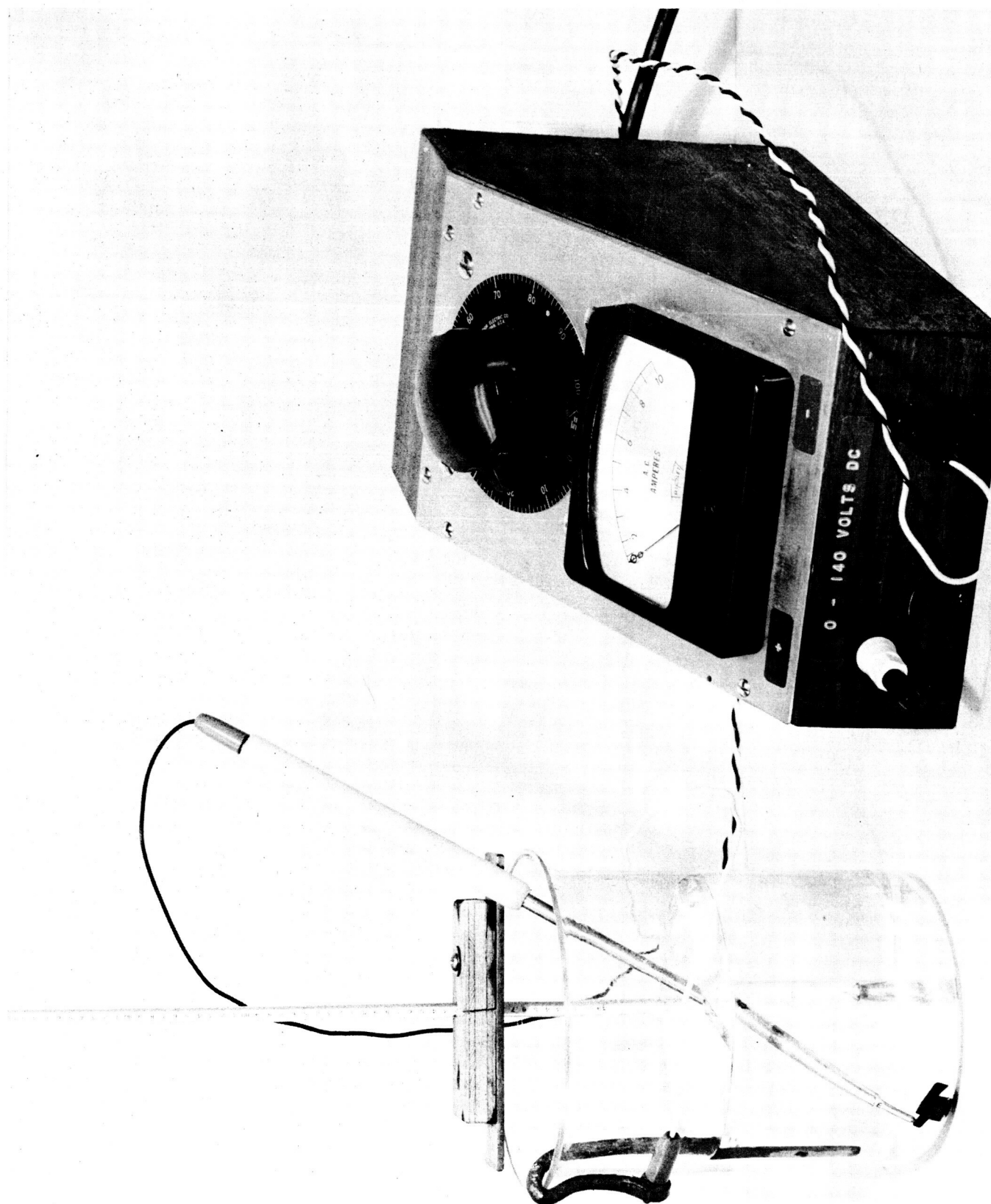


Fig. 1 Technique adopted to clean the anodized aluminum thermopile body (electro-chemical process)

8.b

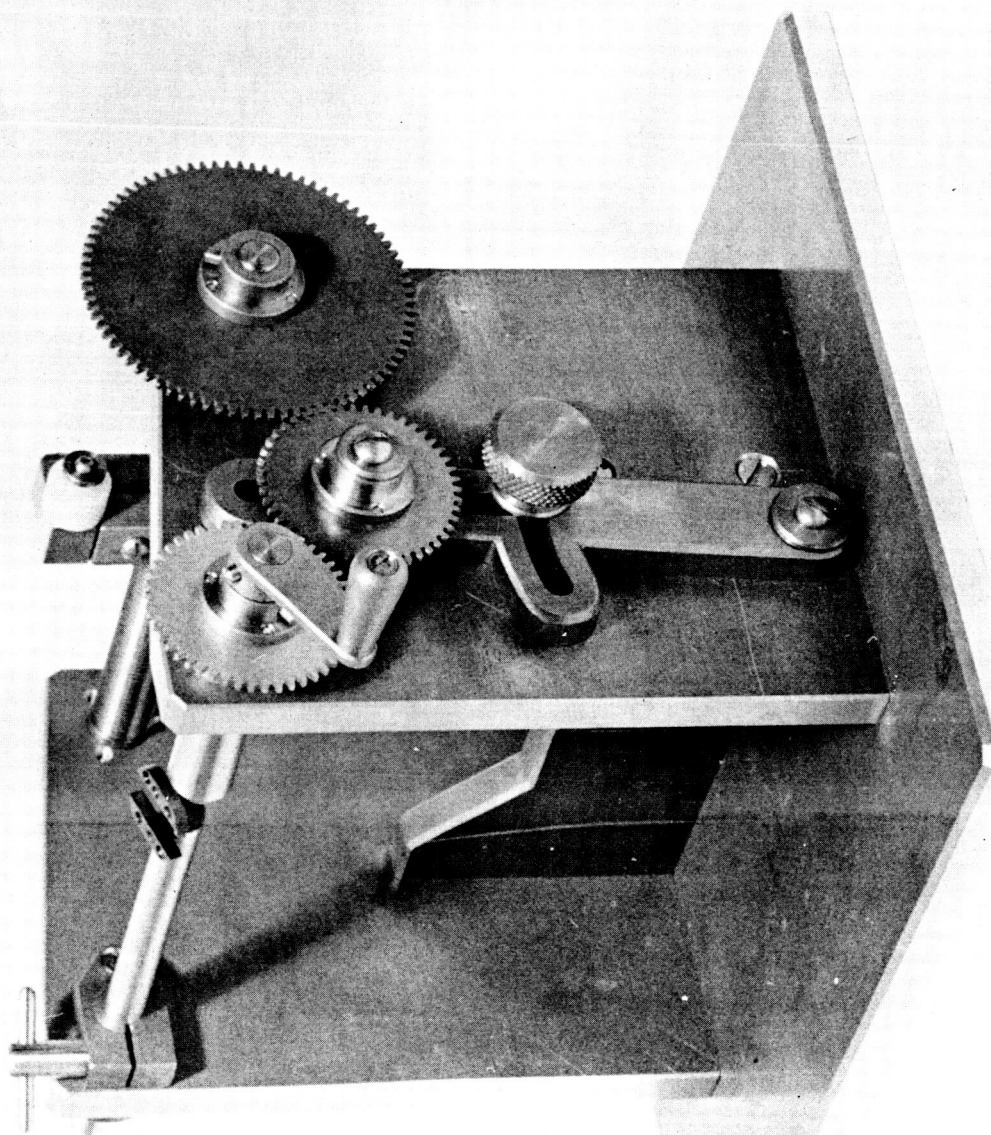


Fig. 2 Apparatus for winding the new type thermopile element

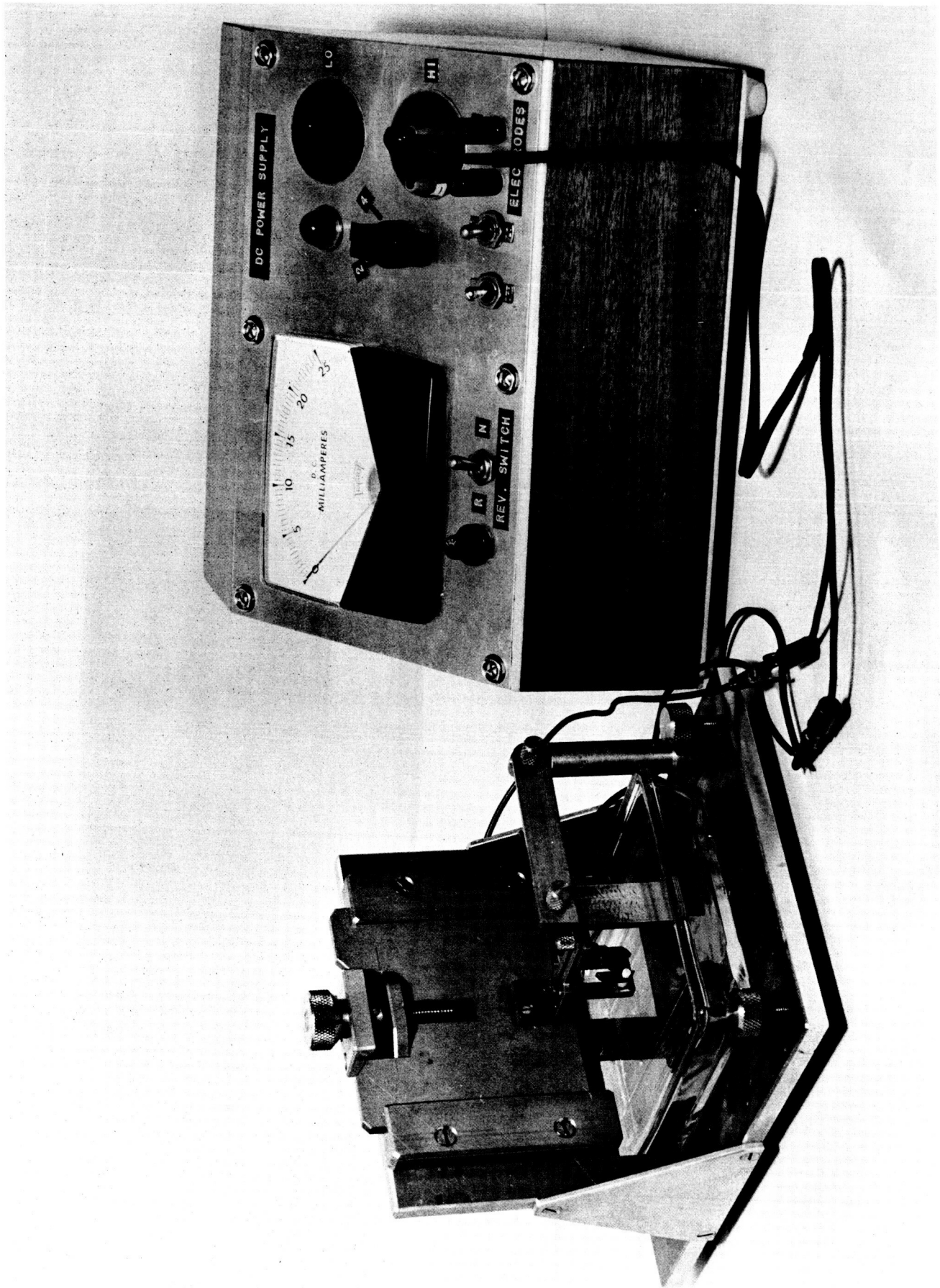


Fig. 3 Apparatus for electro-plating the new type thermopiles

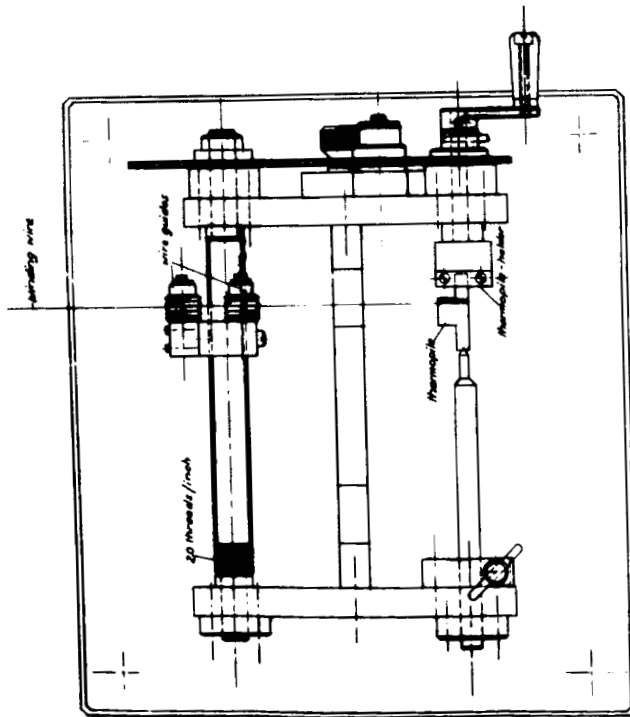
C - 1049 - T.M.

Winding Machine for Artificial Junction Thermopiles

The Engley Laboratory Inc.
Newport B.I. U.S.A

Date: June 1964
by: J. Mueller approved by R. Polster

Scale: Full
Note: For Material and Parts
see Detail Drawings.



Year	1	2	3	4	5	6	7	8	9	10	11	12	13	14	15	16	17	18	19	20	21	22	23	24	25	26	27	28	29	30	31	32	33	34	35	36	37	38	39	40	41	42	43	44	45	46	47	48	49	50	51	52	53	54	55	56	57	58	59	60	61	62	63	64	65	66	67	68	69	70	71	72	73	74	75	76	77	78	79	80	81	82	83	84	85	86	87	88	89	90	91	92	93	94	95	96	97	98	99	100																																																																																																																																																																																																																																																																																																																																																																																																												
1	10	12	14	16	18	20	22	24	26	28	30	32	34	36	38	40	42	44	46	48	50	52	54	56	58	60	62	64	66	68	70	72	74	76	78	80	82	84	86	88	90	92	94	96	98	100	102	104	106	108	110	112	114	116	118	120	122	124	126	128	130	132	134	136	138	140	142	144	146	148	150	152	154	156	158	160	162	164	166	168	170	172	174	176	178	180	182	184	186	188	190	192	194	196	198	200	202	204	206	208	210	212	214	216	218	220	222	224	226	228	230	232	234	236	238	240	242	244	246	248	250	252	254	256	258	260	262	264	266	268	270	272	274	276	278	280	282	284	286	288	290	292	294	296	298	300	302	304	306	308	310	312	314	316	318	320	322	324	326	328	330	332	334	336	338	340	342	344	346	348	350	352	354	356	358	360	362	364	366	368	370	372	374	376	378	380	382	384	386	388	390	392	394	396	398	400	402	404	406	408	410	412	414	416	418	420	422	424	426	428	430	432	434	436	438	440	442	444	446	448	450	452	454	456	458	460	462	464	466	468	470	472	474	476	478	480	482	484	486	488	490	492	494	496	498	500	502	504	506	508	510	512	514	516	518	520	522	524	526	528	530	532	534	536	538	540	542	544	546	548	550	552	554	556	558	560	562	564	566	568	570	572	574	576	578	580	582	584	586	588	590	592	594	596	598	600	602	604	606	608	610	612	614	616	618	620	622	624	626	628	630	632	634	636	638	640	642	644	646	648	650	652	654	656	658	660	662	664	666	668	670	672	674	676	678	680	682	684	686	688	690	692	694	696	698	700	702	704	706	708	710	712	714	716	718	720	722	724	726	728	730	732	734	736	738	740	742	744	746	748	750	752	754	756	758	760	762	764	766	768	770	772	774	776	778	780	782	784	786	788	790	792	794	796	798	800	802	804	806	808	810	812	814	816	818	820	822	824	826	828	830	832	834	836	838	840	842	844	846	848	850	852	854	856	858	860	862	864	866	868	870	872	874	876	878	880	882	884	886	888	890	892	894	896	898	900	902	904	906	908	910	912	914	916	918	920	922	924	926	928	930	932	934	936	938	940	942	944	946	948	950	952	954	956	958	960	962	964	966	968	970	972	974	976	978	980	982	984	986	988	990	992	994	996	998	1000

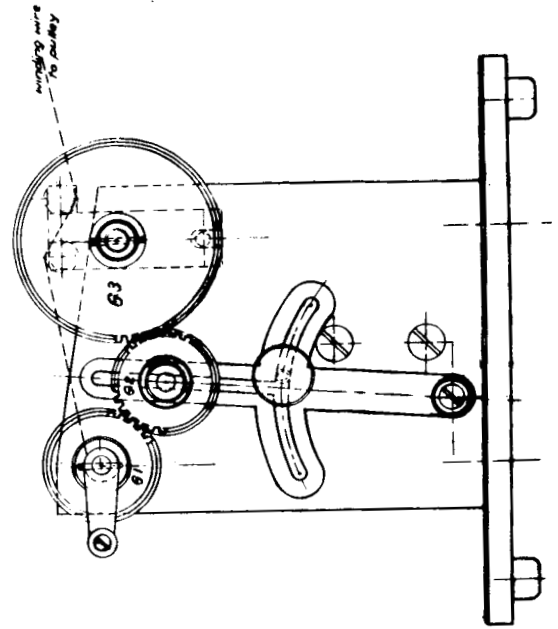
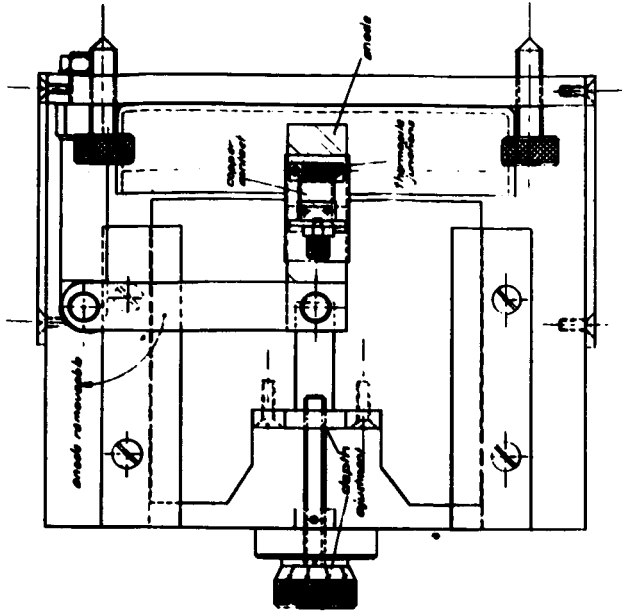


Fig. 4 Diagram of the wire winding apparatus



Plating Bath for Artificial Junction Thermopiles

Score: Full

Note: For Material and Parts see Detail Drawings.

The Eppley Laboratory, Inc.
Newport R.I. U.S.A.

Date: June 19, 1964
By: J. Mueller approved by: R. Friedson

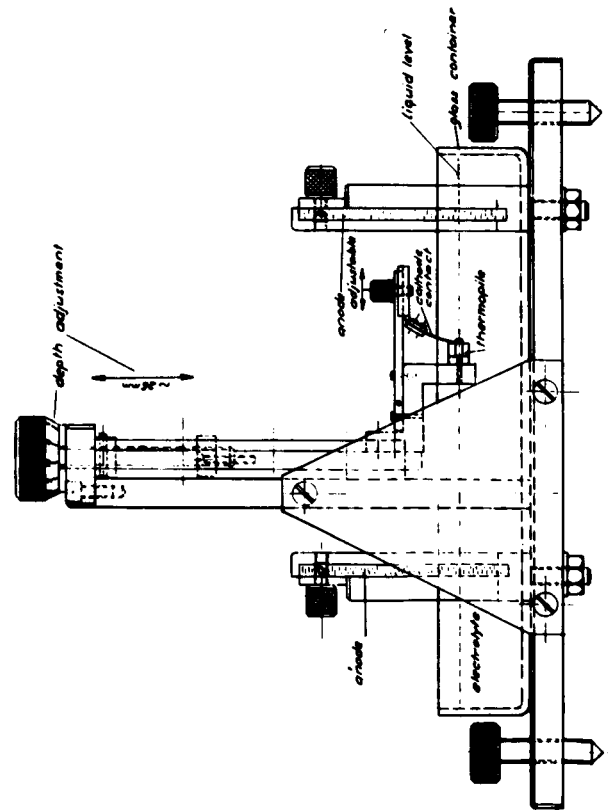
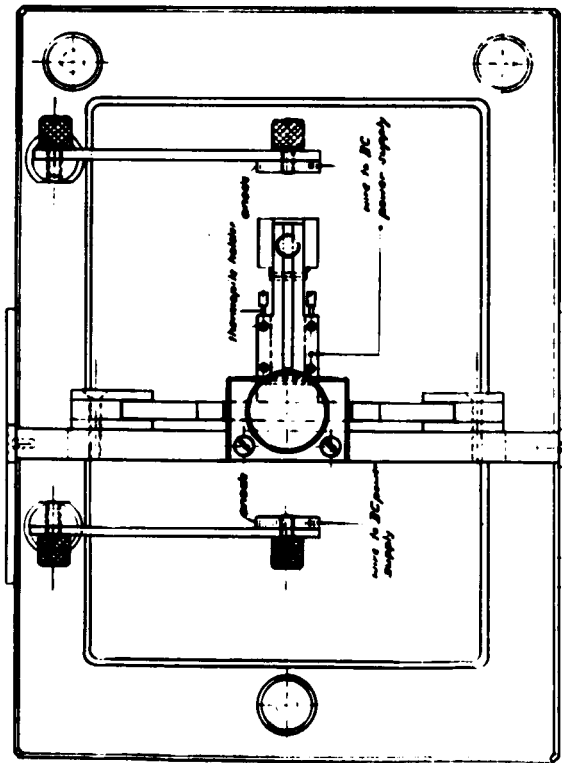


Fig. 5 Diagram of the electro-plating bath

A-1019-T.P.

Power Supply for Electro-Chemical Cleaning Device.

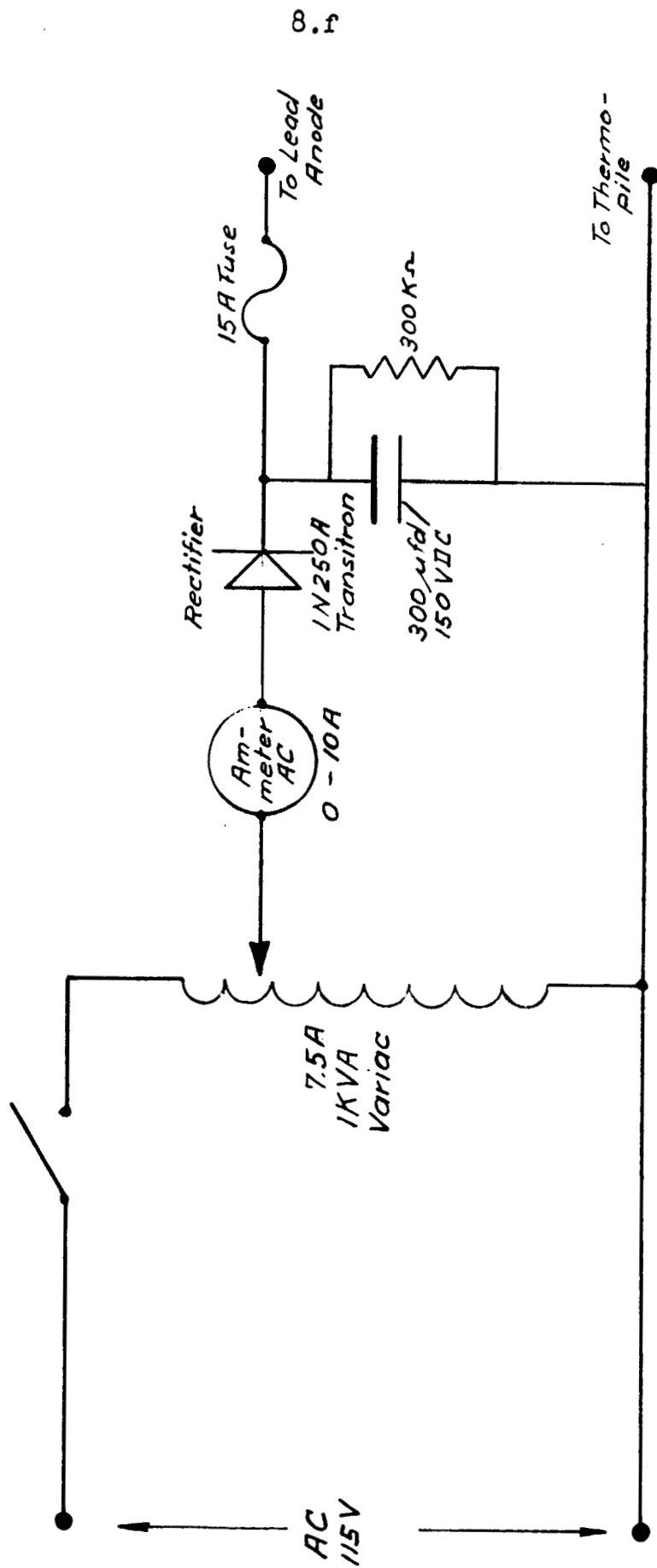
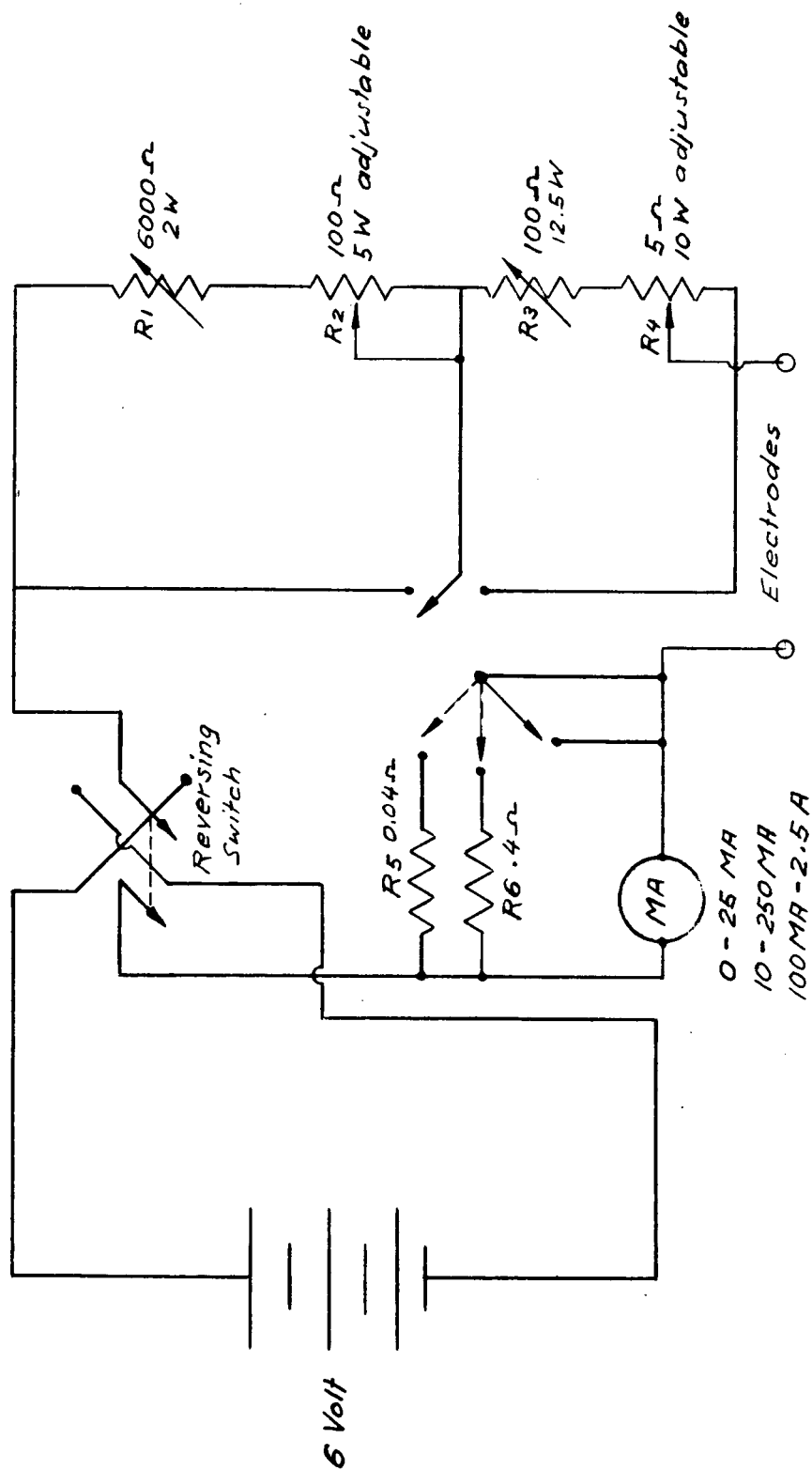


Fig. 6 Schematic diagram of the electrical circuit employed in the control unit of the cleaning apparatus

The Eppley Laboratory Inc.
Newport R.I. U.S.A.

Date: June 1964
by: J.M. apd: R.F.

DC Power Supply for Plating - Bath



8.8

Fig. 7 Schematic diagram of the electrical circuit employed in the control unit of the electro-plating apparatus

The Eppley Laboratory Inc.
Newport R.I. U.S.A.

Date: June 1964

by: J.M. Apd: R.F.

The plating technique (in this first instance, copper - from copper sulfate) developed for this project is believed to be original, the object being to control carefully the deposit thickness, its uniformity and the symmetry of the copper-constantan division. In order to obtain homogeneity of deposition on both top and bottom surfaces of the thermopile windings, two electrodes are immersed in the plating bath, at equal and opposite distances from the unit being plated. The general procedure is as follows: (a) the thermopile unit is so located in the plating bath that, approximately, one-half of the wired surface is immersed in the solution, (b) the current direction for normal plating is reversed and power switched on (roughly 40 ma cm^{-2}), (c) after about 1 minute the current is switched to normal, (d) the plating operation is allowed to proceed for about 10 minutes. After plating, the unit is flushed in distilled hot water. Because of surface tension effects, it is difficult to produce a truly symmetrical straight line of copper-constantan separation and special care, in this respect, is therefore necessary.

The three models so constructed were essentially prototypes; it is felt that, with further development, their performance characteristics will be considerably improved. Experiments (as part of the Eppley Laboratory R and D program in radiometry) are now in progress to examine the possibility of replacing the copper-constantan thermopile element by a similarly electro-chemically deposited one of bismuth-silver (copper). If this approach proves successful (e.g. target: same or better time response and higher sensitivity), then an attack will be made on the production of a germanium-constantan (silver) thermopile which, theoretically, ought to have about ten

times the sensitivity of a copper-constantan element.

Figs. 8 and 9 are schematic diagrams showing the construction principles of models I-III of the new fast-response thermopiles. It will be noticed that this design does not incorporate a solid receiver: the close wire construction constitutes the receiver as, in this instance, the radiation is restricted to normal (or nearly so) incidence and the thermopile operation will be similar to that in calibration. An absorbing coating of (Eppley) lamp-black has been applied.

All three models are of the heat-sink type with anodized aluminum body, as explained. The diameter of the circular receiving wire array (copper-constantan) is 9.5 mm. Provision is made, in the body, for the insertion of a temperature compensator should this be found necessary. All soldering connections were made in accordance with JPL specifications. Details of the construction are as follows:

Model	No. of junctions	Wire (constantan) diameter
I	19	0.08 mm
II	23	0.06
III	40	0.08

2.4 Determination of the performance characteristics of the new thermopile prototypes in air and in vacuum

In the paragraphs which follow in this section of the Report, the following detector aspects are examined:

Sketch of Thermopile - Body for JPL

Contract No. 950929

Models Nos 1 and 2

Material: Aluminum 6061

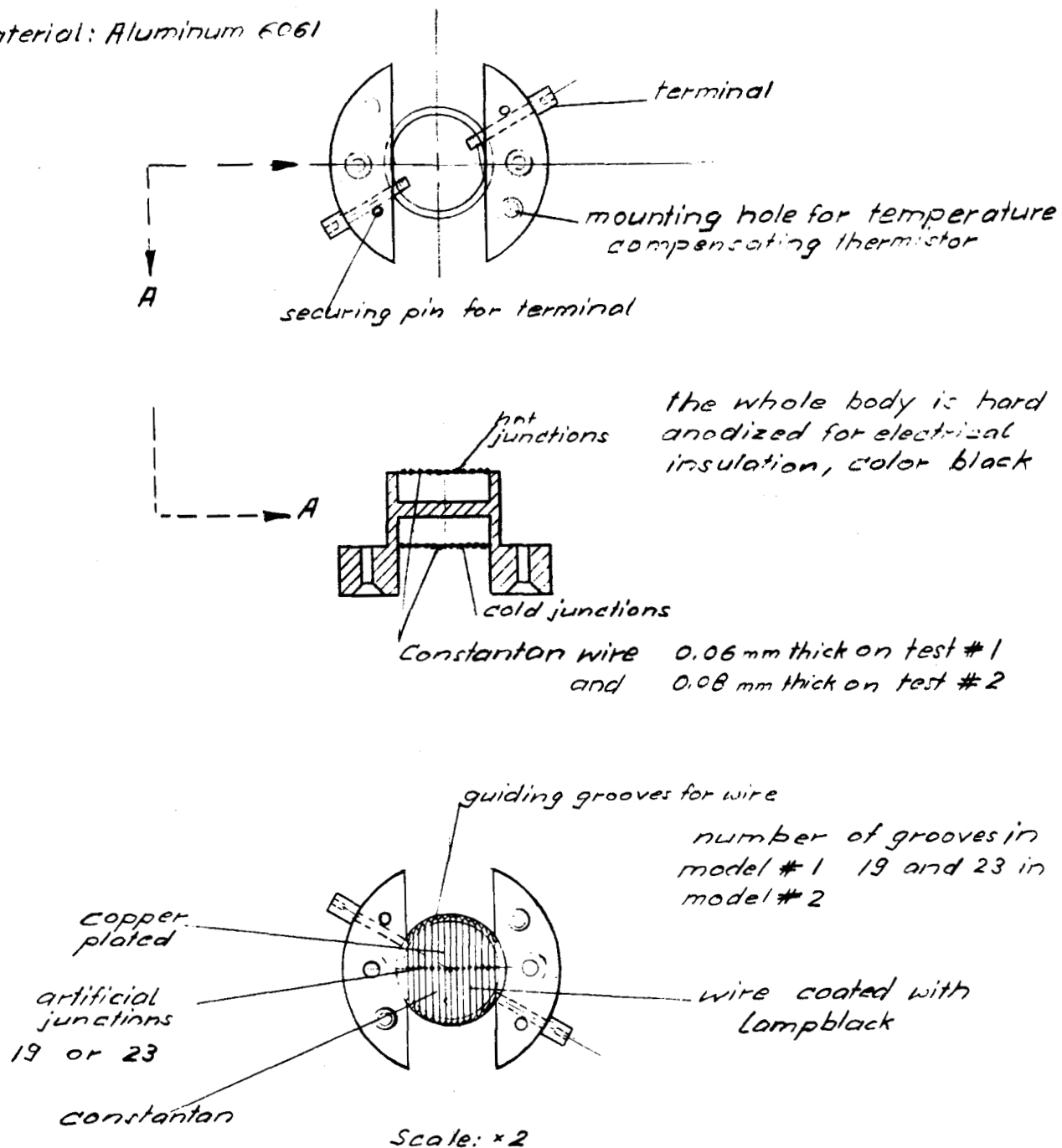


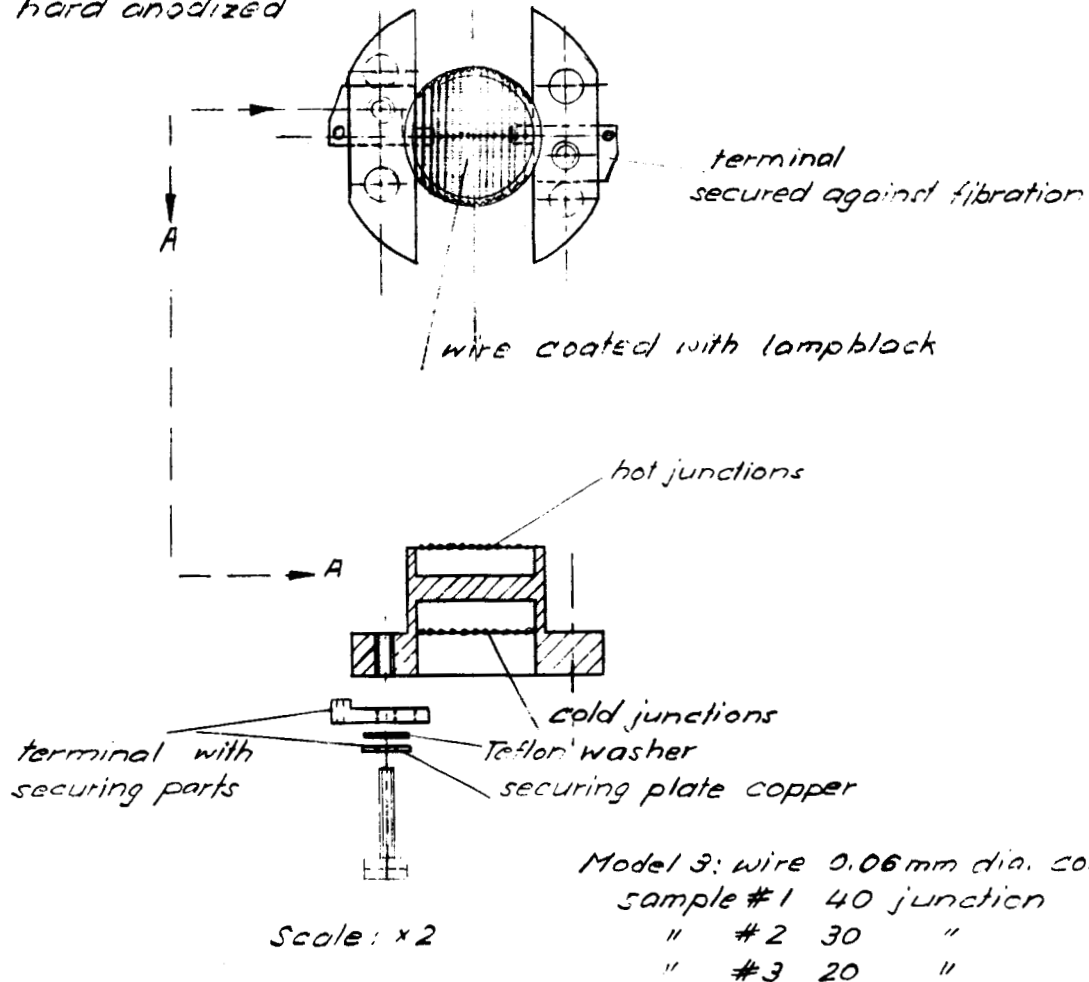
Fig. 8 Diagram showing the construction principle of the new fast-response type of Eppley thermopile (prototype models I and II)

The Eppley Laboratory Inc
Newport R.I

Date: June 18, 1964
by: J.M. Apd: R.F.

Sketch of Thermopile - Body for JPL
Contract No. 950929
Model No. 3

Material: Aluminum 6061
 hard anodized



Shape of grooves in Model No. 3

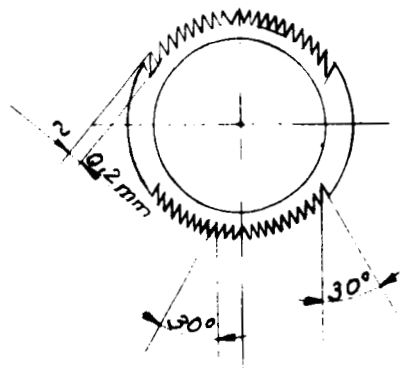


Fig. 9 Diagram showing the construction principle of the new fast-response type of Eppley thermopile (prototype model III)

The Eppley Laboratory Inc.
 Newport R.I.

Date: July 1, 1964
 by: J.M. Apd: R.F.

11.

Time response

Sensitivity, linearity and repeatability

Temperature dependence of sensitivity

Temperature compensation of sensitivity

Wavelength selectivity

2.4.1 Time response

Representative figures are presented in Table III. It will be observed that, for both air and vacuum operation, the time responses of all three prototypes are in the fractional second period for $1/e$ signal. Fig. 10 shows typical oscilloscope records of these measurements.

2.4.2 Sensitivity, Linearity and Repeatability

In Fig. 11 are reproduced the sensitivity curves of the three prototype models, in air and vacuum conditions (see also Table III). In all instances, the degree of linearity (i.e. of the radiometer output versus incident radiation intensity relationship) is very high over a wide range (50 to 200 mw cm⁻²); for example, model II in vacuum shows constancy of better than 1 per cent over the measurement range.

Repeatability of all models is of the order of tenths of a per cent (see Table III).

2.4.3 Temperature dependence of sensitivity

The result of this investigation is such as to indicate that very significant "breakthrough" in thermopile detector design has been accomplished. For instance, in air over a range of ambient temperature of -70 to +90° C (where the normal variation of

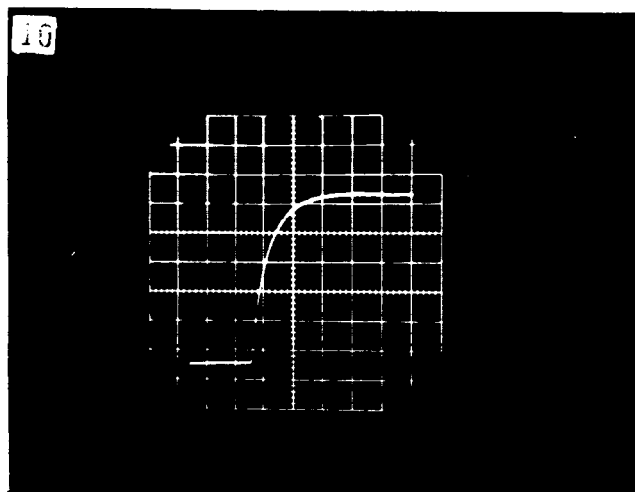
11.a

TABLE III Performance characteristics of the first prototype models
of the new fast-response type of Eppley thermopile

Model	Time Response($1/e$)		Sensitivity(at $2.0 \text{ cal cm}^{-2} \text{ min}^{-1}$)		Repeatability	
	Air	Vacuum	Air	Vacuum	Air	Vacuum
	second		mv/cal $\text{cm}^{-2} \text{ min}^{-1}$		per cent	
I	0.42	0.57	1.35	1.97	99.3	99.1
II	0.38	0.50	1.89	2.58	99.5	99.8
III	0.44	0.70	1.95	3.38	100.0	99.7

N.B. The time required for 98 per cent response is $4 \times 1/e$

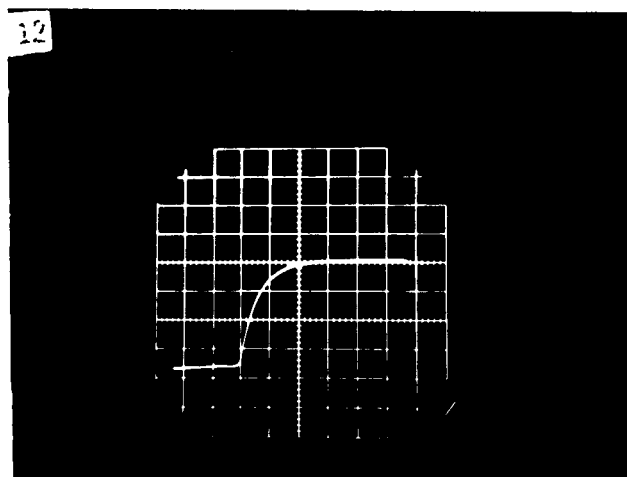
A radiant flux density of $2.0 \text{ cal cm}^{-2} \text{ min}^{-1} = 140 \text{ mw cm}^{-2} =$
 Earth solar constant



TIME RESPONSE IN VACUUM OF MODEL II
SCOPE SETTINGS

HORIZONTAL . . . 1.0 second/cm.

VERTICAL 1.0 millivolt/cm.



TIME RESPONSE IN VACUUM OF MODEL I
SCOPE SETTINGS

HORIZONTAL . . . 1.0 second/cm.

VERTICAL 1.0 millivolt/cm.

Fig. 10 Illustration of the time response of the new Eppley thermopile models, (i.e. $<10^{-4}$ torr), using an oscilloscope with camera attachment

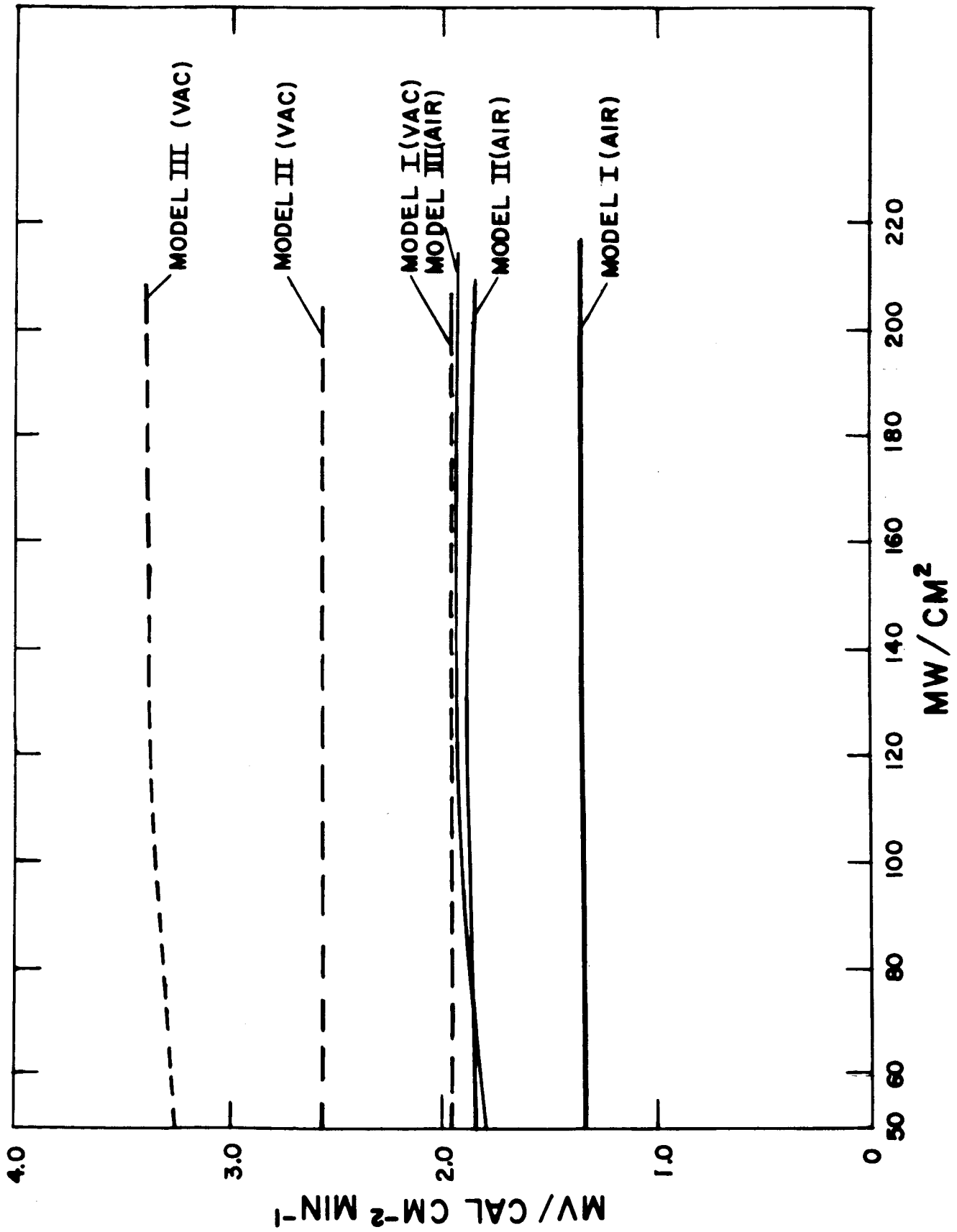


Fig. 11 Sensitivity of the new Eppley thermopile models, in air and in vacuum (i.e. 10^{-4} torr), as a function of radiant flux density - 50 to 200 mw cm^{-2}

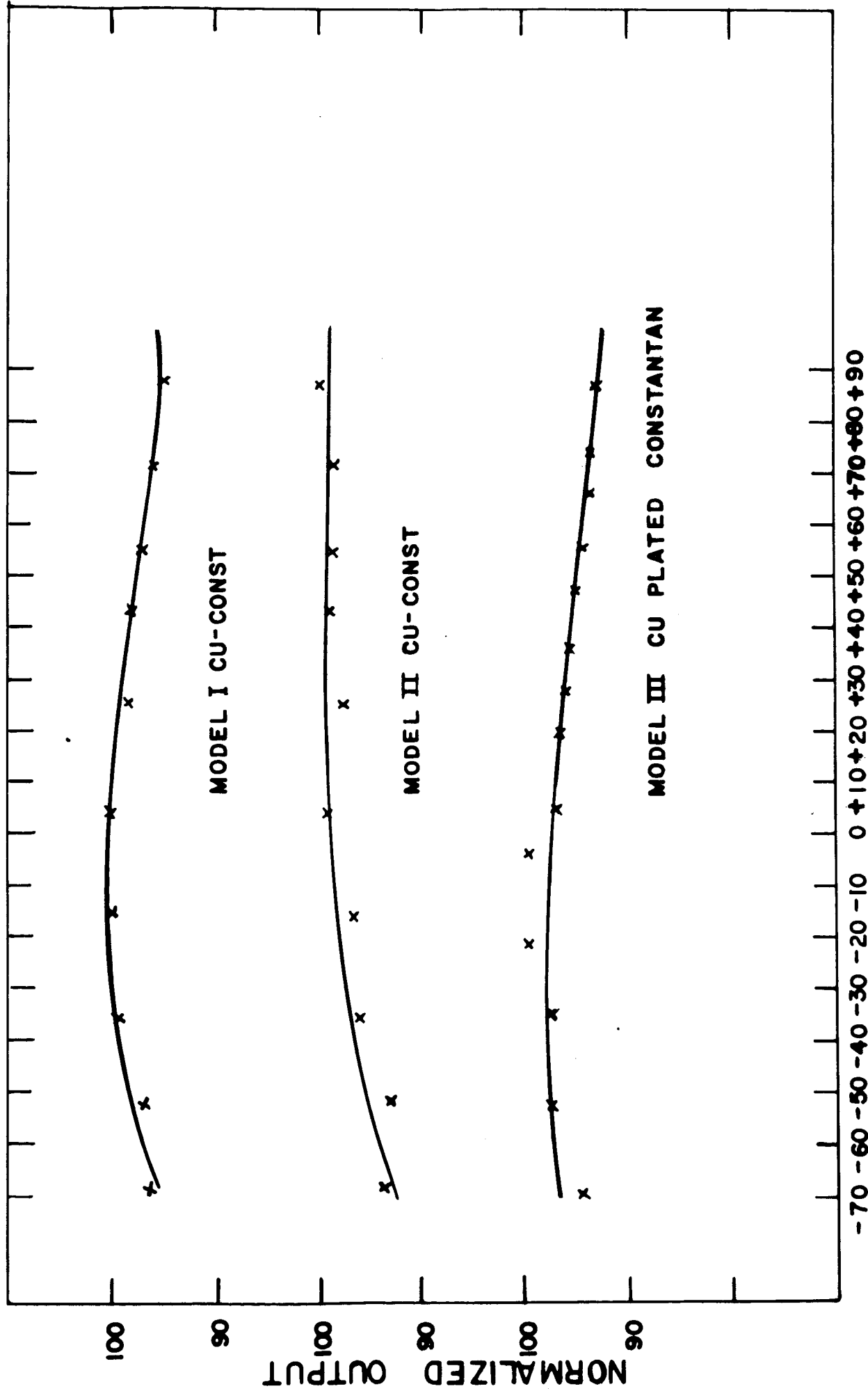


Fig. 12 Temperature dependence of sensitivity of the new Eppley thermopile models in air - ambient temperature range -70 to +90° C

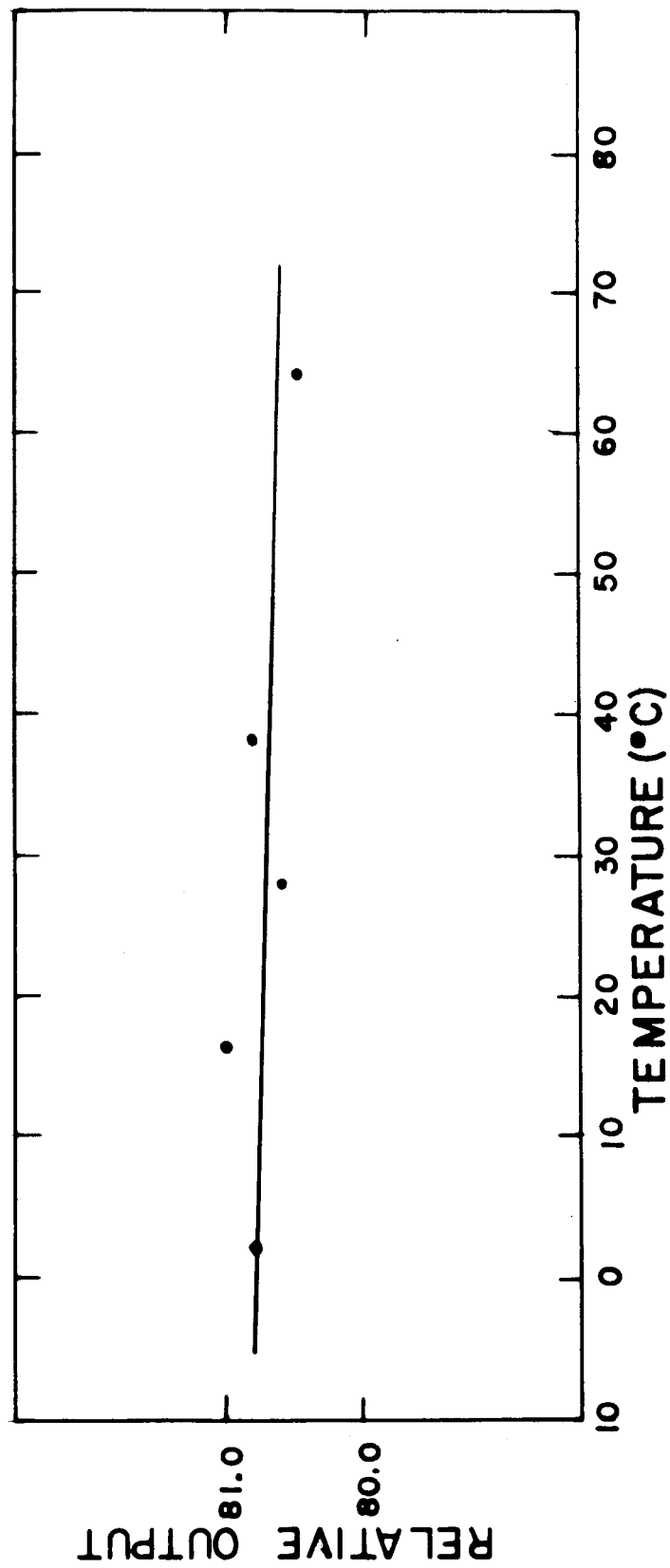


Fig. 13 Temperature dependence of sensitivity of the new Eppley thermopile model III in vacuum (i.e. 10^{-4} torr) - ambient temperature range 0 to +70° C

sensitivity, for a true copper-constantan thermoelement, would be about 35 per cent), the total variation is only of the order of 5-6 per cent. In vacuum, the degree of constancy of detector sensitivity is even higher, e.g. the total variation of the model III unit is no greater than 0.25 per cent over a temperature change of 0 to +70° C. Figs. 12 and 13 are relevant.

2.4.4 Temperature compensation of sensitivity

It is believed that the first realistic attempt at introducing a temperature compensator into the thermopile circuit of a radiometer (pyranometer or pyrliometer) was that described by R. M. Marchgraber and A. J. Drummond⁴. Temperature compensation of radiometer sensitivity was achieved through the use of a bead-in-glass probe type thermistor, shunted by a wire-wound resistor, inserted in series with one of the thermopile leads which were then shunted by a second wire-wound resistor (serving as a fixed voltage dropping resistance in an ideally constant current circuit).

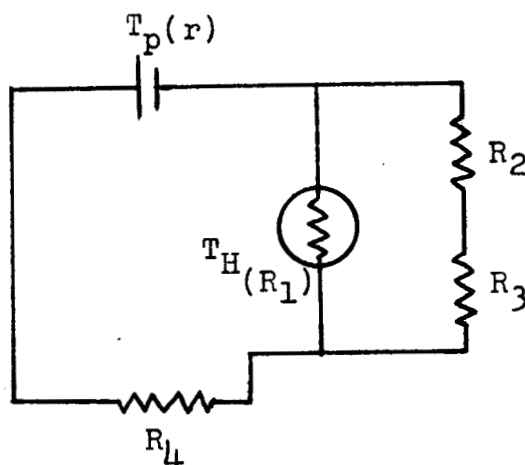
However, this rather simple arrangement has certain limitations; for example, while there is no difficulty in obtaining constancy of radiometer output (for constant radiation flux density) to within ± 1 per cent over the temperature range of -20 to +40° C, extension of these limits entails careful matching of the compensating circuit to the temperature-emf characteristic of the particular thermopile concerned.

A new approach has therefore been made recently. The results of what may thus be regarded as phase II of the Eppley temperature compensation of pyrliometer sensitivity investigation indicate very considerable advancement of this project. It is now

13.

possible to control radiometer sensitivity to better than ± 1 per cent generally (and to within ± 1.5 per cent in the extreme case) over the measured ambient temperature range of -65 to $+50^\circ \text{C}$ (and, by computation, valid for the range -80 to $+55^\circ \text{C}$).

The circuit diagram of the new arrangement for temperature compensation of radiometer sensitivity is as follows



where T_p represents the thermopile sensor (Eppley model 15 A: resistance r), T_H the bead thermistor (Gulton 32PB2 type: resistance R_1), R_2 a precision wire-wound resistor (Precision Resistor Co.) and R_3 and R_4 silicon resistors (Texas Instruments).

The introduction of silicon resistors (greater positive temperature coefficient of resistance as compared with manganin etc.) was suggested by the curvature of the earlier form of the compensated radiometer temperature-output relationship.

The resistances R_1 , R_3 and R_4 were measured with an Eppley Wheatstone bridge (No. 384) at 25 , 35 and 45°C , employing oil immersion.

14.

The temperature dependence of the thermopile sensor of each of the two standard-type normal incidence pyrheliometers investigated was determined in a Tenney environmental chamber, over the temperature range of -65 to $+55^{\circ}$ C.

For this range, the corresponding values of R_1 were computed from the equation

$$R = R_o \cdot e^{\beta \left(\frac{1}{T} - \frac{1}{T_o} \right)}$$

given in Gulton Industries leaflet No. 10M10-57 (page 6), and R_3 and R_4 from Texas instruments leaflet "Transistors and Components" (graphical presentation of resistance change versus ambient temperature).

The voltage (v), for the temperature interval, was computed from the equation

$$V = V_o + V_o \alpha (T - T_o)$$

The appropriate value of R_2 was derived with the aid of Thévenin's theorem, expressed as

$$V_{th} = V \cdot \frac{R_4 (T)}{R_4 (T) + R_o (T) + r}$$

where R_o is the equivalent resistance of the parallel branches and V_{th} is a constant.

The resistance values, at 25° C, of the circuit components of the two pyrheliometers constructed were as follows:

15.

Instrument No.	Thermistor R ₁	Silicon R ₃ R ₄	Wire-wound R ₂	Thermopile r
E. 4899 A	2149	945 3976	600	36 ohms
E. 4900 A	2168	1077 3865	500	36

The temperature compensation of pyrliometer No. E. 4899 A was then tested by exposure to an artificial source in the Tenney chamber.

% Deviation from mean pyrliometer sensitivity
(expressed as mv/cal)

° C	-70	-60	-50	-40	-30	-20	-10	0	+10	+25	+30	+35	+45	Mean
Theor.*		+1.3	+1.0	+0.4	-0.2	-0.5	-1.2	-1.2	-1.0	-0.5		+0.3	+0.7	±0.8
Exp.**	+0.8		+0.5		-0.3		-0.2		+0.3		+0.4		-0.2	±0.4

* for a value for R₂ of 500 ohms

** for a value of R₂ of 600 ohms

Another advantage of this new compensation circuit is increased radiometer sensitivity (as compared with that resulting from the initial compensation circuit): typical values are increased (in this particular investigation) from about 3.5 to 4.5-5.0 mv per cal cm⁻² min⁻¹ (in air).

These paragraphs of the above section of this Report were written prior to the completion of the investigation of the temperature dependence of sensitivity of the new fast-response thermopiles. In the light of the latter findings, the introduction of such

circuitry may not be necessary. However, it is considered advisable at this stage, to include what we think is the basic statement in this respect of thermopile detector sensitivity characteristics.

A detector of the type and construction of the models investigated will exhibit a low temperature coefficient. Since the lowest sensitivity over a given temperature range determines the amount of compensation required, a minimum decrease from the highest possible sensitivity will be experienced. The new thermopile in its final stage of development may not need a temperature compensation circuit. The temperature coefficients of the three types studied vary from positive to negative. This indicates that proper choice of design may eliminate the need for a compensation circuit. If this is not possible for reasons of sacrificing sensitivity or speed, a model which can be compensated by the aforementioned circuitry will be chosen. Study of a method of compensating a detector exhibiting a positive slope (opposite of normal thermopile) is now being conducted in the event that it will be required.

2.4.5 Wavelength sensitivity

As will be seen from Table IV, the new lampblackened detectors are essentially independent in their response with regard to the wavelength of the energy incident upon their receivers, at least over the spectral range of sunlight. However, this aspect of detector sensitivity is not of too great importance to the JPL-Eppley program since due account will be taken in calibration.

2.5 Shock tests

Two rather elementary types of shock test of the new

16.a

TABLE IV Response of the new Eppley thermopile with respect to the wavelength of the incident radiation

Narrow Bandpass Filter No.	Reference Wavelength(m μ)	A		B	
		Reference Thermopile Parsons' black(μ v)	E.3317 New Thermopile (μ v)		A/B
A-5	365	8.0	3.1		2.5
A-8	546	27.2	11.0		2.47
A-10	700	82.0	32.8		2.49
A-12	1500	261.0	111.5		2.34

17.

detector were undertaken. The Eppley facilities did not permit anything more elaborate.

2.5.1 Mechanical

Model III was vibrated (receiving surface, in turn, vertical and horizontal upwards) for two 10-minute continuous test periods at an equivalent gravity acceleration of 23 g simulated by a vertical displacement of 0.20 inch at a frequency of 46 cycles per second. No damage to the detector was observed.

2.5.2 Thermal

Model I was thermally shocked by repeated alternate positioning in a cold environment (refrigerated chamber at a temperature of -70°C) and in a hot environment (oven at a temperature of $+135^{\circ}\text{C}$). No damage to the detector was observed.

3. FILTER RADIOMETRY

3.1 General

The problem in filter radiometry entails the relating of the energy at the receiver of the filtered radiometer to the true energy which exists in the spectral transmittance region of the filter. If the filter exhibited flat transmittance over the emission range of the source, within the filter band, a simple multiplication by the reciprocal transmittance would yield the true radiation emitted in the spectral region sampled. However, most filters do not possess this ideal transmission characteristic. It also must be remembered that the effective bandwidth of a filter limits this approach to relatively wide bands as compared with those of a monochromator. The chosen bandwidth of a filter is based on a compromise between various

factors. These are that (1) sufficient energy will arrive at the receiver to produce a meaningful readout signal in accordance with the sensitivity of the detector; (2) the spectral range of source emission be covered adequately by the filters employed; (3) the filters have no regions of appreciable secondary transmission within the spectral region of source emission; and (4) the transmittance band straddles regions of structured emission spectra as completely as possible. Once the bandwidth of the filter is established, no results of higher wavelength resolution can be obtained. To present the derived spectral data on a common bandwidth basis, averaging over the band is the only method of interpretation in the absence of a known source curve.

Let us consider the essential differences between the two types of filter available for this study, viz. those with (a) narrow and (b) broad bandpass characteristics. In the case of the latter filters, these have sharp "cutoff" (perhaps better termed "cuton") at the lower wavelength limit, with uniform, or nearly so, transmittance throughout the main transmission band. Typical filters of this class have been fully described^{5,6,7}. The lower limit of transparency is usually taken as the wavelength at which the transmittance value is one half of that averaged over the main band. The filter factor, to correct for reflection and absorption losses by the material (generally glass), is clearly a very high approximation to the ideal which is the reciprocal of the main band transmittance. The derivation of such filter factors is, for all practical purposes, independent of the source emission characteristic. The principal

uses of such sharp cutoff broad bandpass filters is thus (a) to separate energy spectrally through differential measurements and (b) to provide checks upon measurements made with narrow bandpass filters isolating wavelength regions within the broad bands of the cutoff filters⁸. The ideal, again, in the case of narrow (interference) filters is that they can be manufactured with closely adhering rectilinear transmittance functions, where the filter factor is of general application. This, however, is not so at present, as is demonstrated in Fig. 26 (which should be studied in conjunction with Fig. 27). Until manufacturing perfection is realized in the production of narrow bandpass filters, interpretation of radiometric measurements under such filters involves, for best accuracy, an iteration process which matches the derived readings with a series of assumed source emission curve shapes. This essentially consists of varying the slopes and intercepts of straight line sections (e.g. on the graphical presentations) until close adherence between assumed radiometer output and measured output is achieved.

3.2 Specific requirements for the JPL-Eppley project

The provisional selection of wavelength intervals (10) to be isolated by filters in this experiment is given in Table V. As will be seen there (and as indicated earlier in this Report) the emphasis is upon the spectral region below 500 mμ and, to a lesser extent, upon that around 1.5 μ.

3.3 Filter development

In connection with the JPL-Eppley Solar Spectral Measurement Experiment, a research program has been initiated with the

19.a

TABLE V Provisional selection of wavelength intervals (10) to be isolated by filters in the JPL-Eppley Solar Spectral Measurement Experiment

<u>Filter No.</u>	<u>Wavelength Interval(mμ)</u>
1	<300
2	300 - 350
3	350 - 400
4	400 - 450
5	450 - 500
6	500 - 600
7	>500
8	>700
9	1400 - 1800
10	not decided (probably below 300 mμ)

N.B. Filters Nos. 1-6, 9 and 10 will be narrow bandpass (interference) type and Nos. 7 and 8 will be sharp cutoff broad bandpass type.

purpose of developing optical bandpass filters with improved characteristics. The wavelength positions of the bands will have preassigned values lying within the spectral region 250-2500 μ . It is planned that this program will be conducted continuously over the period 1 July - 31 December 1964.

The broad objective of this R and D program is that of achieving (a) maximum possible transmission within the band, (b) steepest possible slope of the filter profile (i.e. sharpest delineation of filter bandpass) and (c) minimum possible secondary transmission. Important considerations guiding the program are:

1. The background rejection must extend over the free filter range of the Eppley thermopile detectors as exposed to the true or an artificial sun (i.e. essentially the spectral range 200-3000 μ).
2. The energy rejected must be mainly, if not entirely, reflected in order to minimize heating of the filter (with consequent emission into the detecting system).
3. The materials employed, both substrate and thin film, must be chosen to minimize solarization effects.

The greatest need for improved filters is in the UV-near visible region 200-400 μ . This spectral region has therefore been selected as the starting point of the study. In the sub-region 200-300 μ it is necessary to assemble the filter components with annular spacer rings: organic cements (epoxies) which would provide a more solid package must be avoided on account of their tendency to absorb, partially or totally, energy of wavelength shorter than 300 μ . The substrates which will be used for the 200-300 μ region are

21.

quartz of high purity. The materials used in such filter manufacture will be pure aluminum and cryolite. The filters are and will be of the Fabry-Perot type and will be described in detail later. Periodically, as the work progresses, samples will be tested at the Eppley Laboratory and then forwarded to JPL for further tests (especially for environmental survival).

3.4 Filter examination

A total of 8 spectrophotometer tests were made on 7 UV filters, with air environment.

3.4.1 Spectral transmittance with special reference to primary and secondary bandpass characteristics

See Figs. 14-21. Remarks: need to increase primary transmittance - secondary transmittance sufficiently suppressed.

3.4.2 Spectral transmittance with special reference to angle of incidence of radiation

See Figs. 14-17. Remarks: provided that the angle of incident radiation to narrow bandpass filters does not exceed 5° from normal, the effect on filter transmittance so introduced may be neglected, for all practical purposes (in the case of broad bandpass filters this effect is definitely less and is mainly determined by specular reflectance at the glass surface).

3.5 Shock tests

- | | | |
|--|---|----------------------------------|
| 3.5.1 <u>Mechanical (air-vacuum)</u> |) | In the time available it was not |
| 3.5.2 <u>Solarization (UV radiation)</u> |) | possible to separate these two |
| | | types of test. |

In Figs. 22-25 are reproduced transmittance curves of

SERIAL NO. ANGLE TEST OF FILTER U.V. 2037
 SLIT 575-500 (Monochromator glass)
 SCANNING TIME Actual 51.5
 DATE _____

SPECTRACORD
 THE PERKIN-ELMER CORP.

SAMPLE _____
 SOLVENT _____
 CONC. _____
 CELL _____

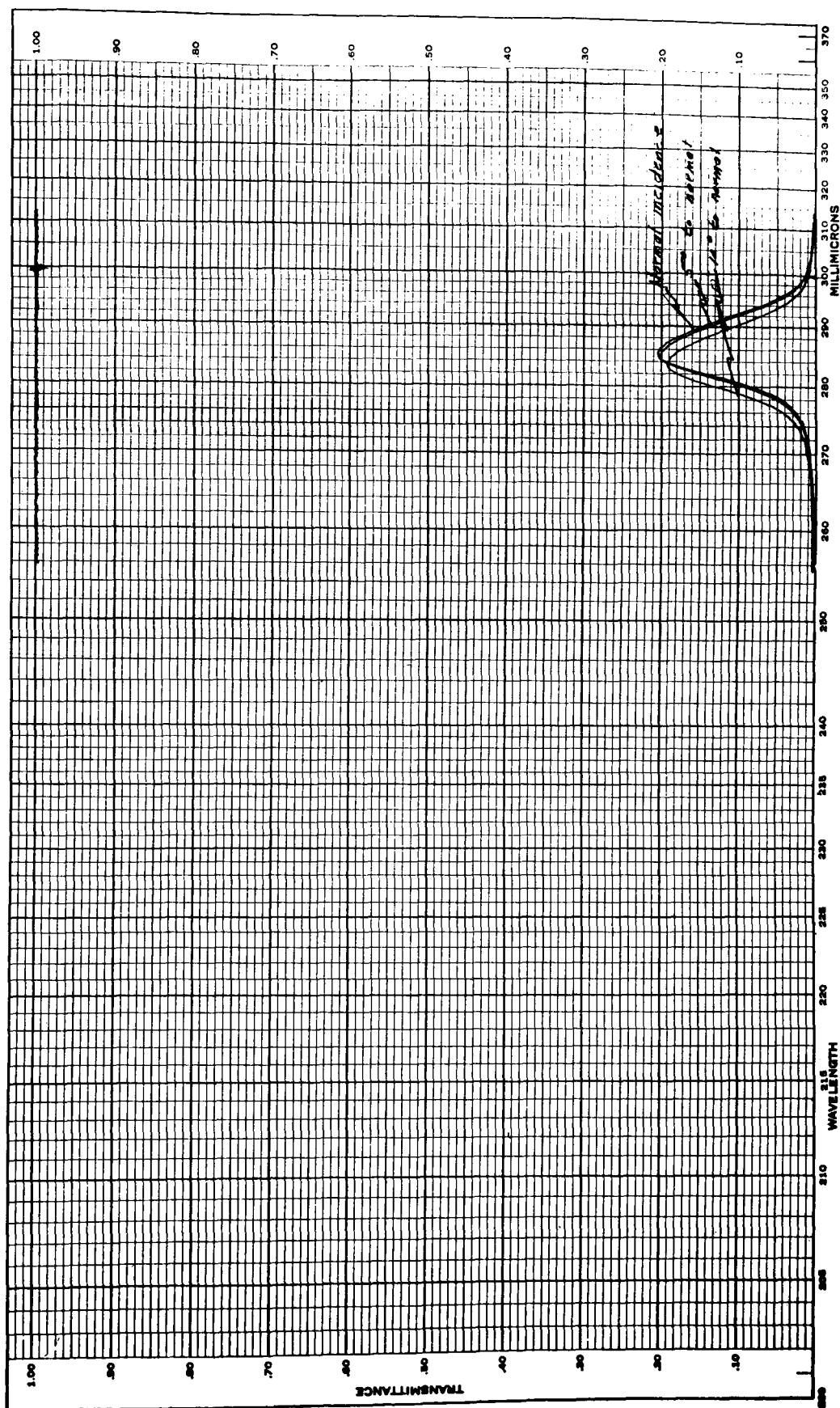


Fig. 14 Spectral transmittance of a typical narrow bandpass (i.e. interference type) filter in the middle UV region for (a) normal incidence radiation and (b) when tilted 5 and 10° to normal - actual scale

SERIAL NO. ANGLE TEST OF FILTER U.V. 2027
 SLIT 2.25-300 (Absorbance scale)
 SCANNING TIME EXPANDED SCALE
 DATE JULY 10 1964

SPECTRACORD
 THE PERKIN-ELMER CORP.

SAMPLE _____
 SOLVENT _____
 CONC. _____
 CELL _____

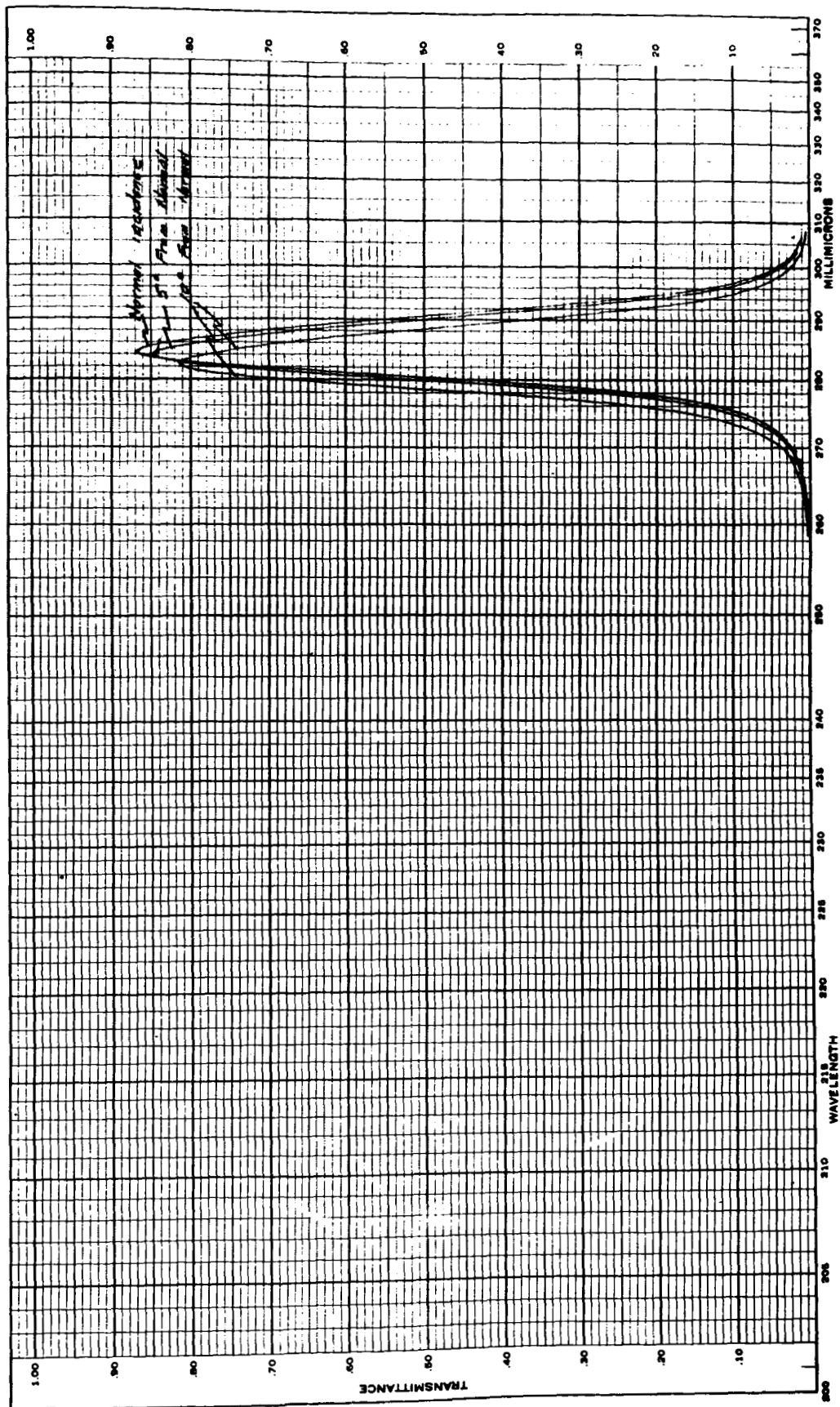


Fig. 15 Spectral transmittance of a typical narrow bandpass (i.e. interference type) filter in the middle UV region - expanded ordinate scale

SERIAL NO. ANGLE TEST OF FILTER U.V. 2037
 SLIT 250-300 EXPANDED SCALE
 SCANNING TIME _____
 DATE 10 JULY 1964

SPECTRACORD
 THE PERKIN-ELMER CORP.

SAMPLE _____
 SOLVENT _____
 CONC. _____
 CELL _____

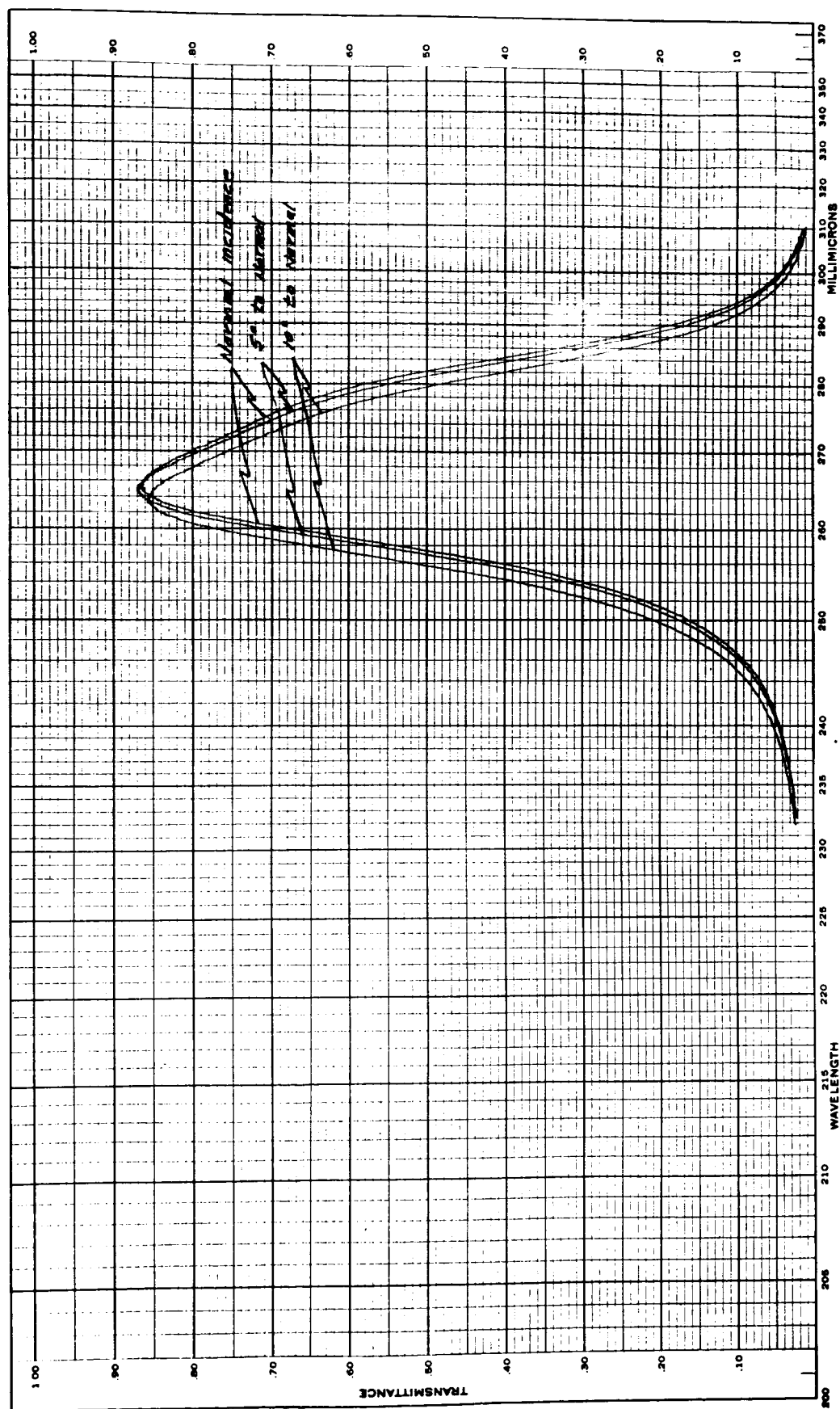


Fig. 16 Spectral transmittance of a second typical (broader limits) narrow bandpass filter in the middle UV region - expanded ordinate scale

SERIAL NO. ANGLE 72- of Filter U.V. 2037
 SLIT 0.2 mm (for RMC Spec)
 SCANNING TIME 6 MINUTES
 DATE July 19 1964

SPECTRACORD
 THE PERKIN-ELMER CORP.

SAMPLE _____
 SOLVENT _____
 CONC _____
 CELL _____

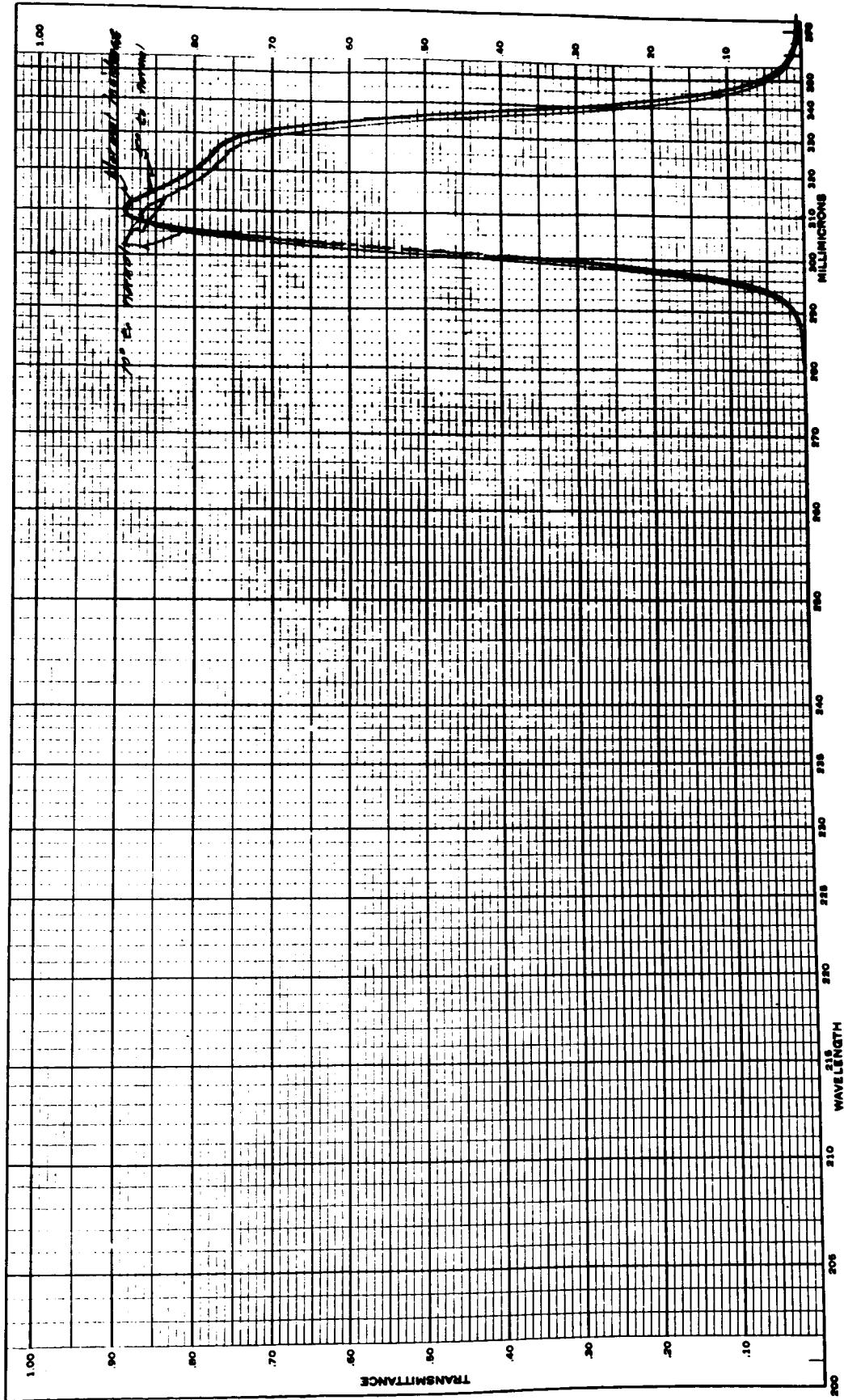


Fig. 17 Spectral transmittance of a third typical narrow bandpass filter in the near UV region - expanded ordinate scale

SPECTRACORD
THE PERKIN-ELMER CORP.

SAMPLE _____
SOLVENT _____
CONC. _____
CELL _____

SERIAL NO. SECONDARY OF 7
SLIT FIGURES FOR UPL
SCANNING TIME SCALE EXPANDED 210 TIMES
DATE JULY 10 1964

VIS. 2798

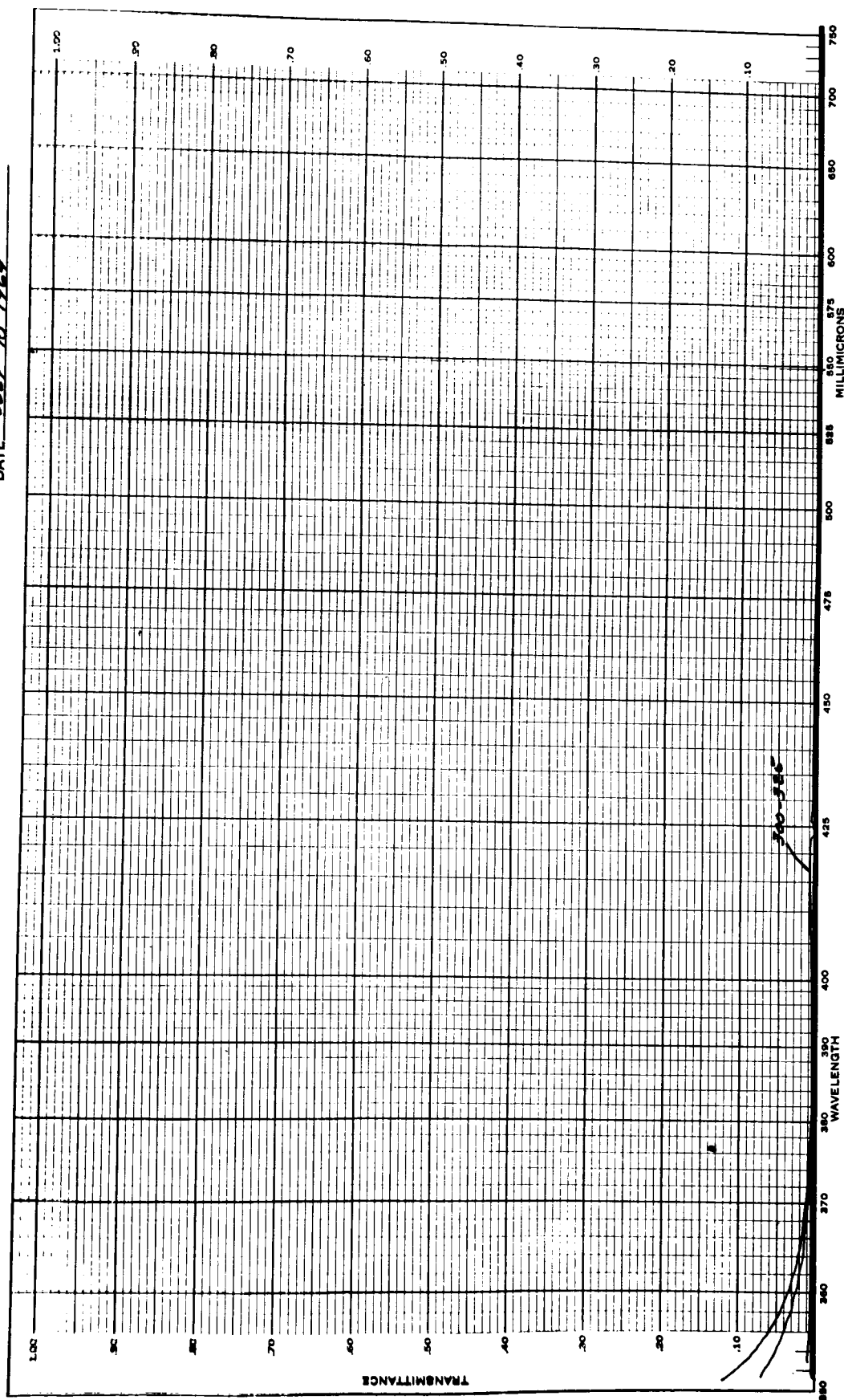


Fig. 18 Secondary transmittance of 7 typical UV narrow bandpass filters (including the 3 filters of Figs. 14-17) in the visible region: primary bandpasses 250-300, 275-300, 300-325 and 300-350 mμ - ordinate scale expanded $\approx \times 10$

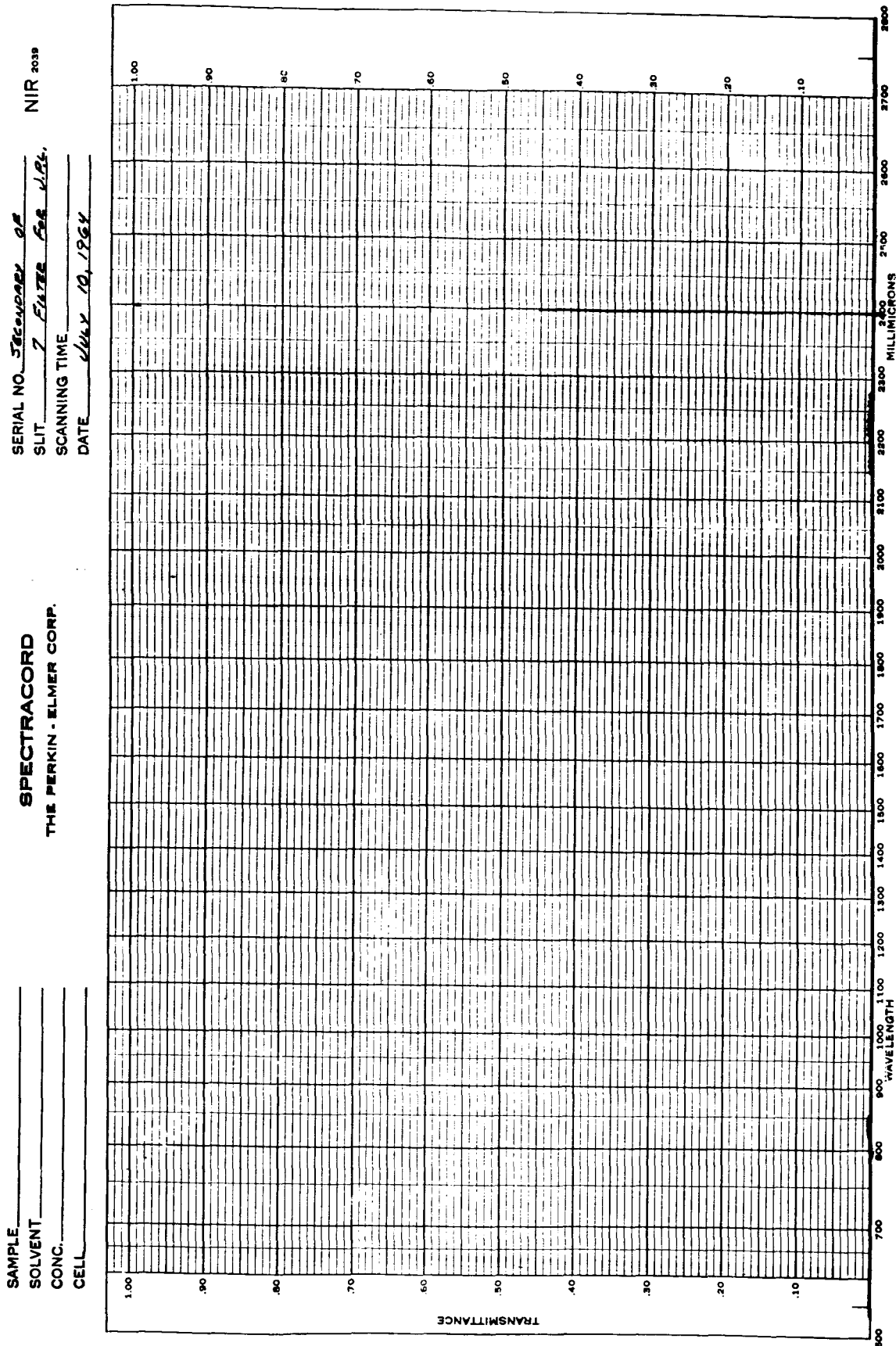


Fig. 19 Secondary transmittance of 7 typical UV narrow bandpass filters (including the 3 filters of Figs. 14-17) in the near IR region: primary bandpasses 250-300, 275-300, 300-325 and 300-350 μ - ordinate scale expanded $\approx \times 10$

SERIAL NO. FILTERS FOR MRL VIS. 2038
 SLIT EXPERIMENTAL (SATURATE)
 SCANNING TIME _____
 DATE 24 JULY 1964

SPECTRACORD
 THE PERKIN-ELMER CORP.

SAMPLE _____
 SOLVENT _____
 CONC. _____
 CELL _____

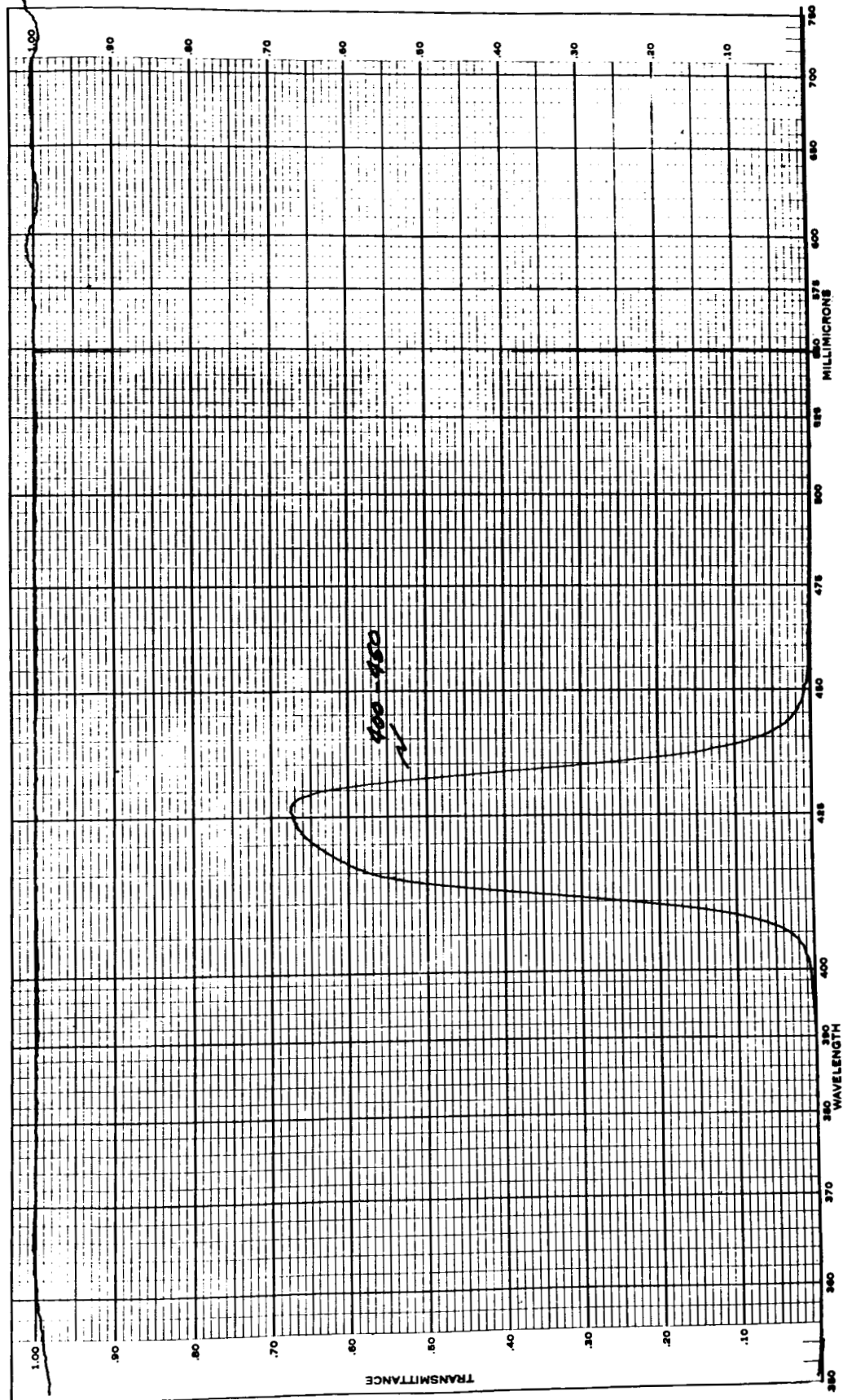


Fig. 20 Spectral transmittance of a typical narrow bandpass filter in the visible region - actual scale

SAMPLE _____
SOLVENT _____
CONC. _____
CELL _____

SPECTRACORD
THE PERKIN - ELMER CORP.

SERIAL NO. FILTERS FOR VPL NIR 2039
SLIT EXPERIMENTAL (SAFETY)
SCANNING TIME _____
DATE 24 JULY 1964

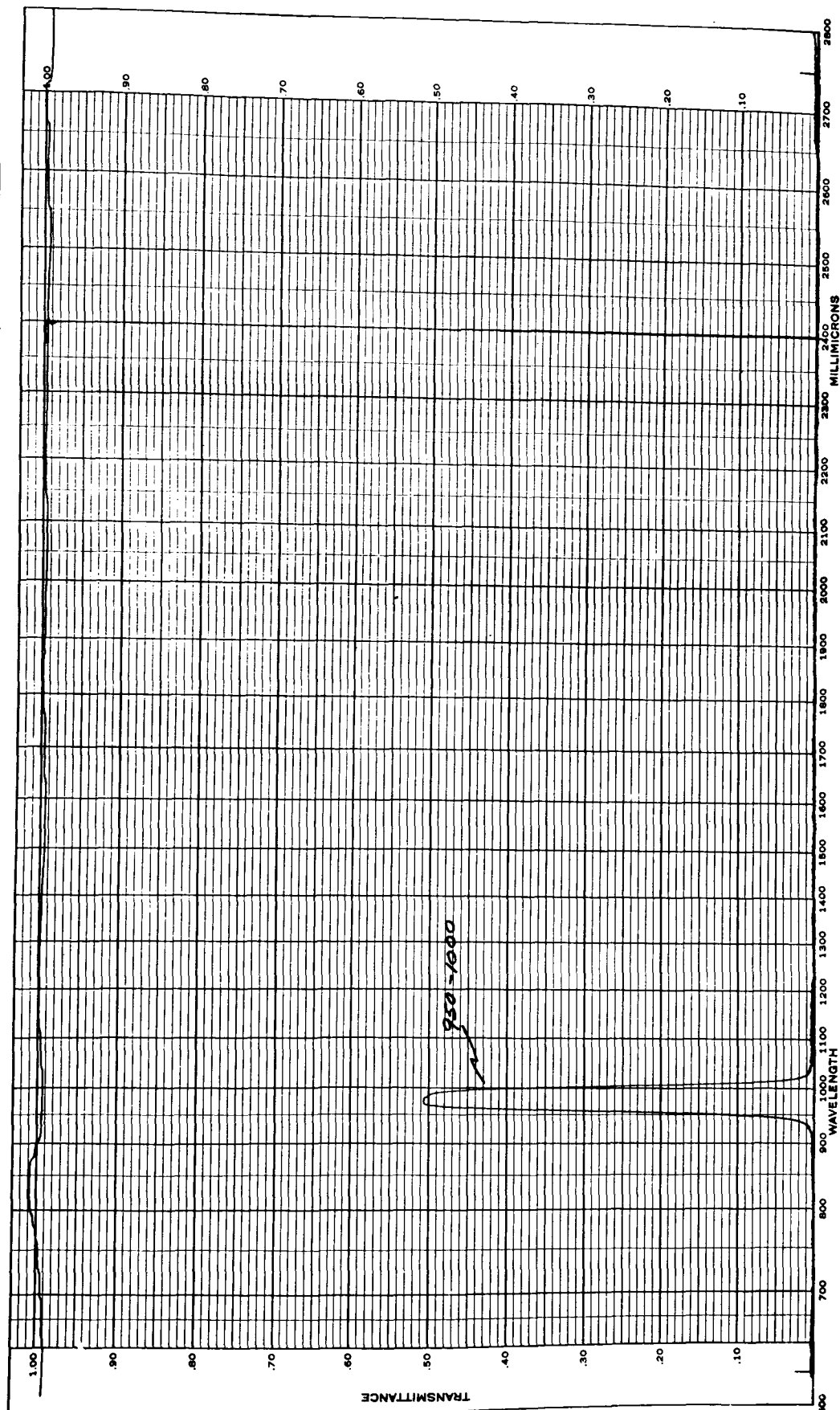


Fig. 21 Spectral transmittance of a second typical narrow bandpass filter in the near IR region - actual scale

SERIAL NO. FILTER Feb 1964 U.V. 2037
 SLIT SLIT (SATURATE)
 SCANNING TIME _____
 DATE 10 JUN 1964

SPECTRACORD
 THE PERKIN-ELMER CORP.

SAMPLE _____
 SOLVENT _____
 CONC. _____
 CELL _____

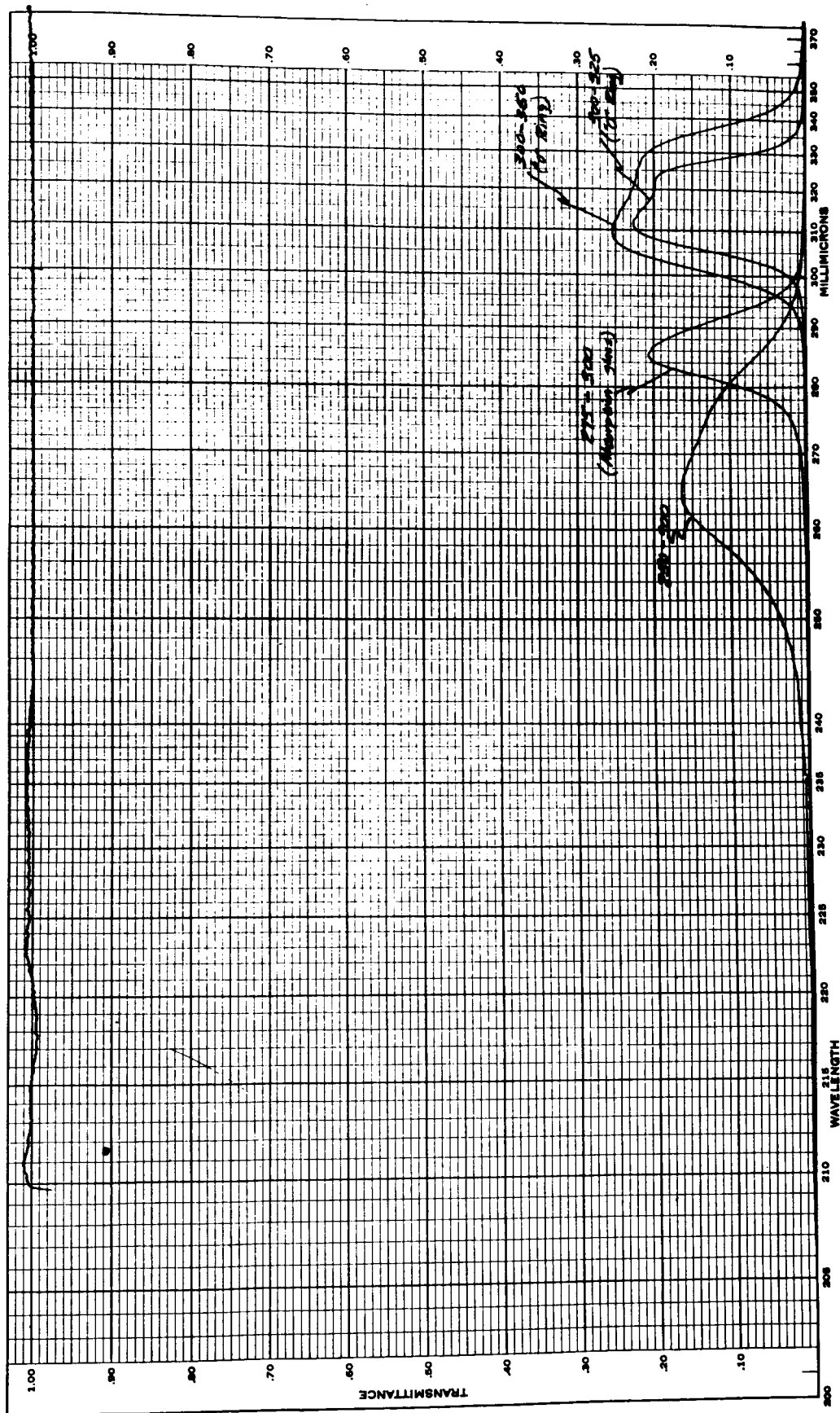


Fig. 22 Spectral transmittance of a first series of 4 UV narrow bandpass filters before exposure, in a vacuum system, to UV radiation - actual scale

SPECTRACORD
THE PERKIN-ELMER CORP.

SAMPLE _____
SOLVENT _____
CONC. _____
CELL _____

SERIAL NO. Filters for V.P. Exp (SA 44.72)
SLIT After exposure to UV (in vacuum)
SCANNING TIME For 24 hr
DATE July 22, 1964

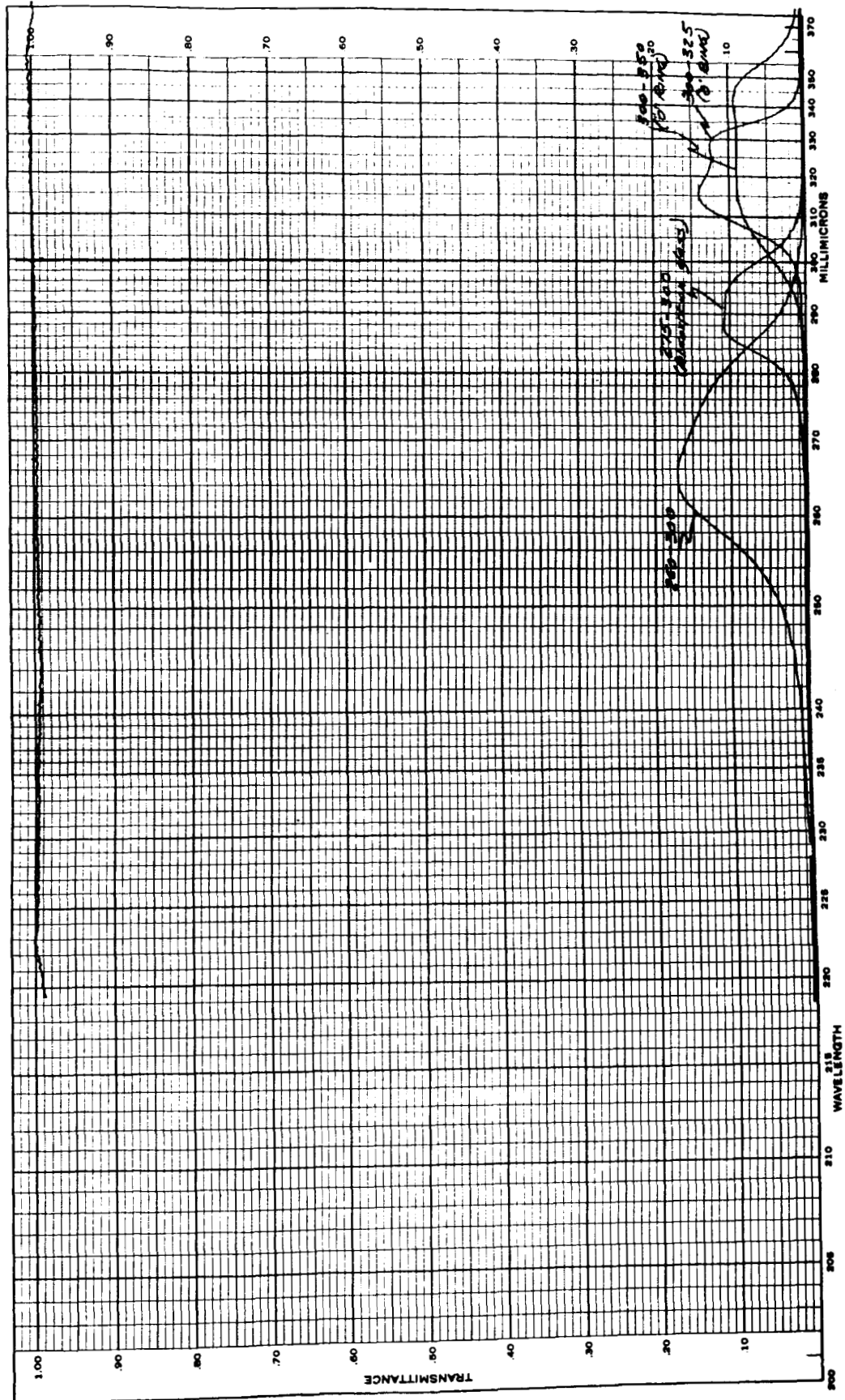


Fig. 23 Spectral transmittance of a first series of 4 UV narrow bandpass filters after exposure, in a vacuum system, to UV radiation - actual scale

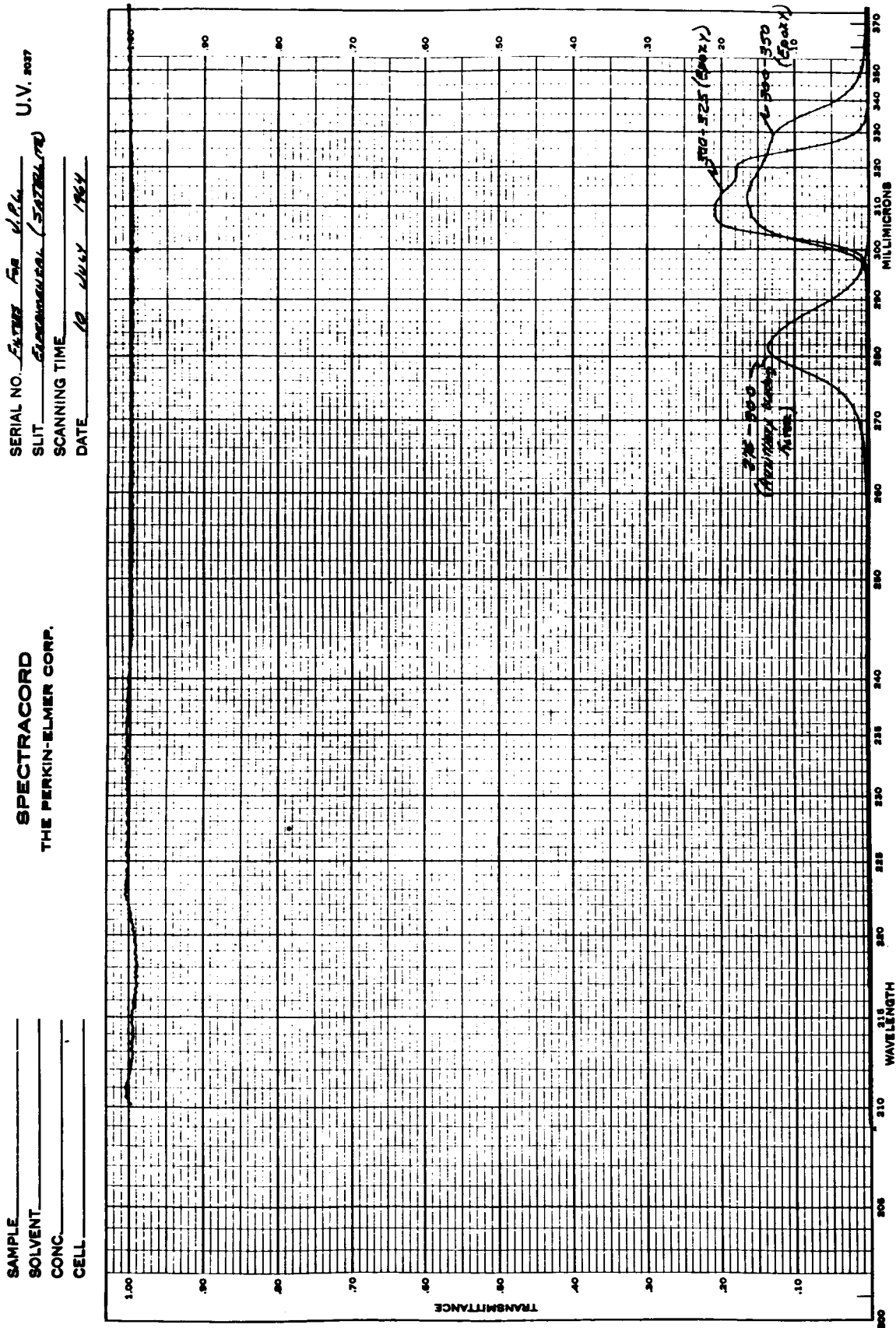


Fig. 24 Spectral transmittance of a second series of three UV narrow bandpass filters before exposure, in a vacuum system, to UV radiation - actual scale

22.

7 filters isolating UV bandpasses (a) before exposure, in a vacuum system, to UV radiation and (b) after 24 continuous hours of such exposure: the radiant flux density at the test plane was, approximately, 25 mw cm^{-2} of which roughly one-half was UV radiation.

There was no effect on epoxy bonded filters; where "O" ring spacers were employed, there was significant deterioration of filter transmittance. This has to be investigated further (see Section 3.3). Indication that this was a mechanical (air-vacuum) effect was supported by a simple test involving the immersion of one sample of each filter type in boiling water: there was no effect on the epoxy bonded filter, whereas the "O" ring spaced filter leaked water markedly.

4. DETECTOR SIGNAL OPTICAL AMPLIFICATION

4.1 Choice of lens

It is obvious from the considerations of the small amount of radiation arriving at any detector equipped with a UV filter and exposed to the extraterrestrial solar beam that a small output voltage will be presented to the amplifier unit. In order to increase this signal, the detector should be submitted to as large a flux as possible. To increase the flux level, lenses will be employed for the purpose of collecting the solar energy over a larger area than that of the detector receiver. Discounting the transmittance of the lens, the ratio of focused to unfocused irradiance will be approximately the ratio of the lens area to that of the detector area. The true optical amplification will be computed using radiometric techniques. The lenses will be of high grade quartz of the

23.

best optical quality. The intensity distribution of the focused beam at the plane of the thermopile should have a distribution which will give maximum sensitivity without loss of detector speed. Based on the assumption that a uniform irradiance at this plane will be the most satisfactory condition, simple lenses will be the first to be tested.

It is doubtful that all filtered detectors will be equipped with lenses since satisfactory signals will be obtained without such amplification for some channels. Lenses of varying speed may be necessary for different channels in order to achieve outputs above the minimum, but below the maximum accepted by the amplifier.

Lenses chosen for use will be studied for aberrations and corrected for those which will impair their use in this application. It is felt that chromatic aberration will not present a problem since the wavelength band will be limited to small sections of the spectrum. Spherical aberrations will present more of a problem and will be investigated.

The physical and optical characteristics of the lenses will be investigated to assure that no distortion of the radiometric results will occur under flight conditions.

In order to further conserve the available energy transmitted by the filter, an antireflection coating may be applied to the lenses. This coating will be "tuned" to a wavelength near the center of the channel's spectral band.

The effects of diffraction, as experienced in the image of a distant point source, will also be investigated.

4.2 Lens tests

The preliminary lens tests consist of the measurement

of focal length, and an inspection of the image of the sun as produced by the lens. A special test jig has been constructed so that a small optical bench unit may be mounted on an equatorial mount at the Eppley Laboratory observatory. Using this apparatus, all final lens tests may be made in the solar beam. Radiometric tests will include measurements of focused and unfocused solar flux using both conventional and the new type thermopile elements. The uniformity of flux at the proposed measurement plane will be sampled using photoelectric or photovoltaic cells with a very small field stop at this location. Photographic means may also be employed to evaluate the image.

Laboratory tests of the lenses will include the usual optical bench tests to determine the lens characteristics. These tests will not be considered as important as the radiometric tests but will be used to check the reproducibility in manufacture of a designated lens type.

Thus far four lenses have been received for test. All are plano-convex. Two of these lenses had focal lengths longer than the proposed depth of the final radiometer channel and were discounted for possible use. The second two lenses are being evaluated presently. The power of these lenses is closer to the estimated limit of 20 diopters than the previous two samples. The focal lengths are 6.57 cm and 7.37 cm. Both lenses exhibit some spherical aberration, but the amount has not as yet been determined. The lenses received thus far are to be used only to evaluate the methods in general and do not necessarily constitute a choice of lens type. Experience gained in testing these two lenses will guide the design study for the final lens

type. Field angles and stop positions will be calculated to assure the proper transfer from calibration to use.

5. CALIBRATION PROCEDURES FOR DETECTOR SYSTEMS

5.1 In sunlight

The basic reference of thermal radiation, at relatively high intensity, is the International Pyrheliometric Scale (1956) with the sun as source. It is believed that this proposal represents the true radiation reference to within ± 1 per cent and, possibly, ± 0.5 per cent.

At the Eppley Laboratory this fundamental reference is reproduced by a group of 4 \AA electrical compensation pyrheliometers which are compared periodically at international geophysical institutes.

5.2 In the laboratory

Here the problem is one of transfer. The results of a calibration of 6 detectors, using two different methods of calibration are given in Table VI. The mutual consistency of the results averages at ± 0.25 per cent.

However, in the case of filter measurements, where flux values of low (filtered) intensity have to be compared with much higher ones of total flux, it is essential, for best accuracy, that the detector linearity characteristic be established - see section 2.4.2 above.

The low intensity radiation scale is the NBS scale. The carbon filament lamp is the transfer standard from the original blackbody calibration. The irradiance at 2 meters distance is

25.a

TABLE VI Examples of the mutual consistency of Eppley high-intensity thermopile calibrations: solar-laboratory transfer (air operation)

June 1964 Radiometer No.	Source: Integrating Hemisphere Calibration in mv/mw cm ⁻²	Source: Optical Bench Calibration in mv/mw cm ⁻²
E. 5954-A	0.114	0.1135
E. 5955-A	0.1175	0.1185
E. 5956-A	0.1195	0.1185
E. 5960-A	0.1245	0.125
E. 5961-A	0.117	0.116
E. 5997-A	0.121	0.121
Mean	0.1189	0.1887

Notes

1. The reference meteorological-type radiometer employed in the integrating hemisphere (powered by 24 tungsten lamps: approximately 5 KVA) is calibrated by periodic exposure, under natural conditions of sunlight, to the working standard radiometer (pyranometer, i.e. 180° pyrliometer) which, in turn, is calibrated using the Eppley group of primary standard pyrliometers (normal incidence: Ångström electrical compensation type).
2. The reference laboratory-type thermopiles (2) employed on the single 5000-watt lamp-powered optical bench (i.e. directional source) are calibrated through comparison, on the bench, with a normal incidence pyrliometer which, in turn, is calibrated, in sunlight, against the above-mentioned Eppley group of primary standards.

25.b

3. The radiant flux levels, at the test planes, are about 60 mw cm^{-2} in the integrating hemisphere and $50\text{-}100 \text{ mw cm}^{-2}$ on the bench.
4. The six radiometers reported on in the above table are pyranometers (i.e. 180° pyrhemliometers) of the Mark I type incorporating removable twin hemispherical envelopes of quartz. All calibrations tabulated here were made, in air, with the envelopes in position.

26.

varied from approximately $40 \mu\text{w cm}^{-2}$ to $100 \mu\text{w cm}^{-2}$ by changing the lamp current. These calibrations are for total radiation only. In order to check the agreement of the IPS and NBS scales a triple transfer method is necessary. First a thermopile detector is calibrated at low intensity using the carbon lamp standard. This same detector is then used to establish the intensity level at the far (approximately 3.5 to 4 meters) end of the high intensity calibration bench. The source for this test bench is a 3200°K , 5000 w, tungsten filament, projection lamp. Since for some types of thermopiles the sensitivity varies with intensity, the transfer to this bench test must be made at a level close to that of the carbon lamp value. Also a correction must be made for the difference in spectral distribution of the two source emissions. Using a quartz window, a total filter factor of 1.084 is applied for tungsten and a factor of 1.19, 1.20 or 1.21 for carbon for lamp currents of 350, 300 or 250 ma. Once the lower limit of the high intensity bench is established, the inverse square law is used to determine the irradiance distribution up to a distance of one meter from the lamp. The calibration is then extended to higher intensity by moving the thermopile to a position at which the irradiance is in the range of the solar irradiance at the earth's surface. The thermopile is then fitted with a tube which matches its field of view to that of the \AA ngström pyrheliometer and is calibrated in the observatory laboratory against the standard instruments (or a normal incidence pyrheliometer which has been recently calibrated). The calibration value is then checked against the value obtained during transfer on the high intensity bench.

Sometimes absolute measurements referenced to the IPS scale are made of the high intensity bench source. This measurement is more difficult than those outlined previously due to aperture conditions caused by using an extended near source rather than a distant point source such as the sun.

Although this transfer measurement technique involves at least three difficult measurements, agreement between the scales has been shown to be about $\pm 2\%$. Considering the difficulty of transfer, the actual agreement is probably better than this. Further tests are being devised to check this agreement with a minimum of experimental error.

The spectral standards employed at this laboratory at present are the standards of spectral radiance. Calculation of irradiance at a given distance in any given spectral band between $0.25\ \mu$ and $2.5\ \mu$ is possible if a suitable system of stops and apertures is employed. A filter of known transmittance can be employed to separate the desired band. The irradiance in any band is usually very small when the detector aperture system is arranged properly. However, low irradiance levels of known spectral quality can be obtained using this method.

6. DETERMINATION OF DETECTOR (HEAT SINK) TEMPERATURE

This presents no problems. There are two obvious (well proven) choices; viz. platinum resistance thermometry or the thermistor-bead probe approach, to the D.C. electrical bridge method. The present study suggests an ambient temperature measurement accuracy as lenient as $\pm 10^\circ\text{C}$, so the technique to be adopted, for

28.

this aspect, is of secondary consideration.

7. ACKNOWLEDGEMENTS

The following Eppley personnel participated in the preparation of this Design Study:

A. J. Drummond (Project Director)
J. R. Hickey (Deputy Project Director)
R. Frieden
H. W. Greer
F. Griffin
J. Mueller
J. J. Roche
W. J. Scholes
J. Warner

In addition, thanks are due to R. M. Barnett and E. G. Laue, of the Jet Propulsion Laboratory, for assistance mainly through stimulating discussion.

8. REFERENCES

- 1 J. Meteor., 11, 431, 1954
- 2 Archiv Meteor., Geoph., Biokl., A, 3, 209, 1951
- 3 Annales d'Astrophys., 14, 249, 1951
- 4 Marchgraber, R. M. and A. J. Drummond: International Radiation Symposium, Oxford, July 1959
- 5 Ångström, A. K. and A. J. Drummond: J. Meteor., 18, 361, 1961
- 6 Hickey, J. R., D. A. Brett and A. J. Drummond: Tellus, 14, 451, 1962
- 7 Hickey, J. R.: "A Study of Radiometric Filters". Thesis, University of Rhode Island, 1962
- 8 Hickey, J. R. and A. J. Drummond: "Measurement of Simulated Solar Radiation with Special Reference to Spectral Determination". CIVRES, Paris, July 1964

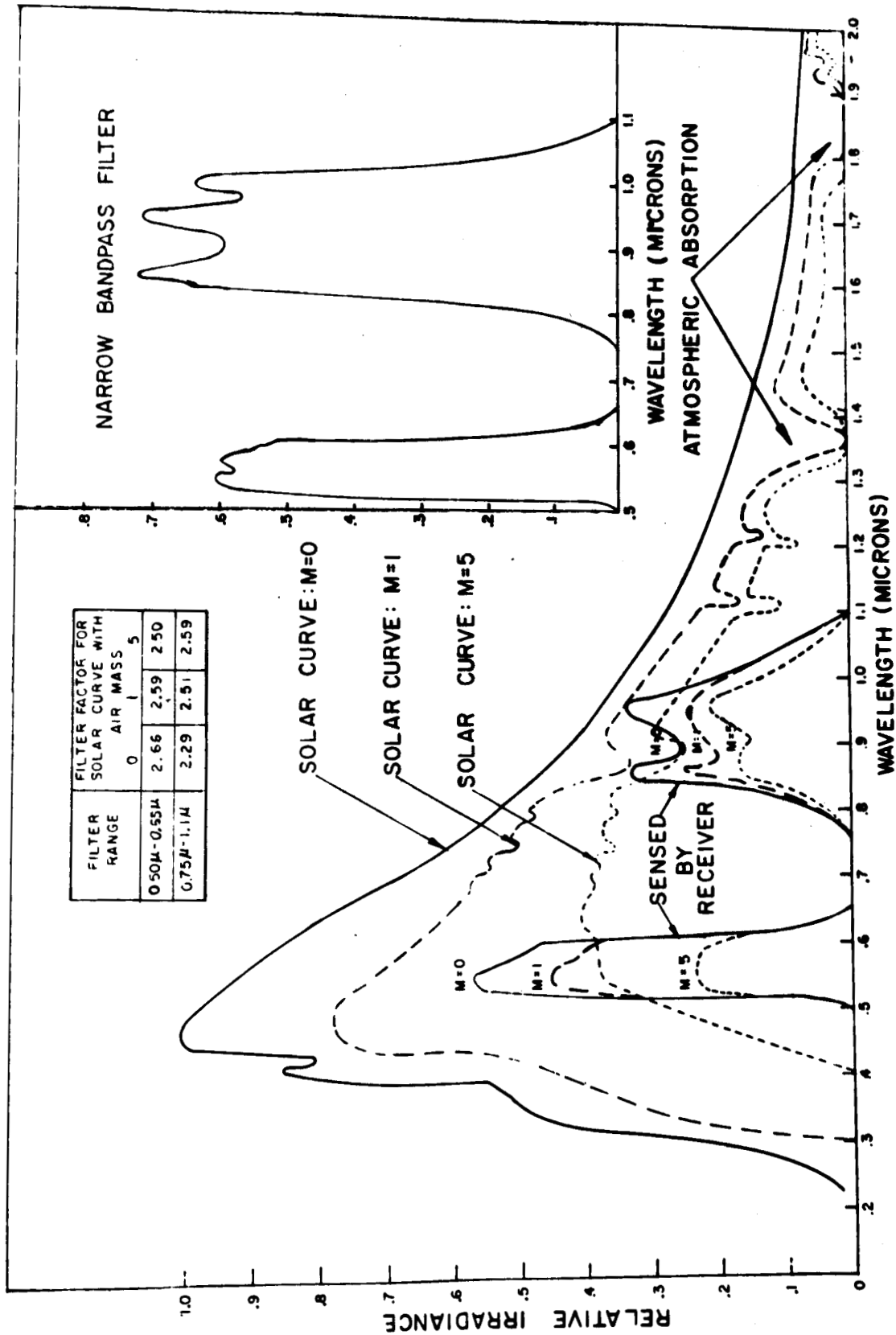


Fig. 26 Examples of the dependence of the filter factor for narrow bandpass selectivity on source emission characteristics (solar optical air mass = 0, 1 and 5)

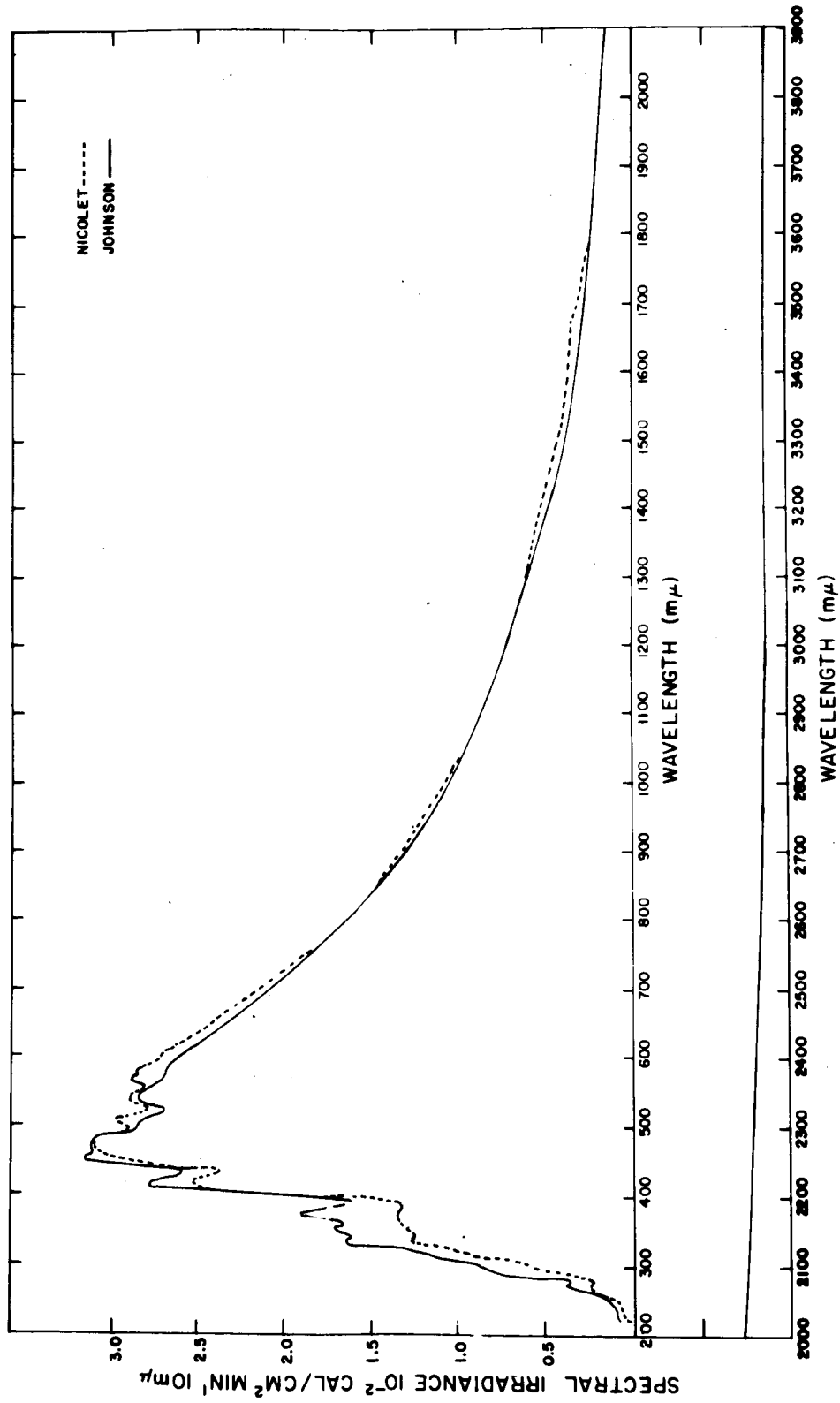


Fig. 27 The spectral distribution of the extraterrestrial solar radiation, according to (a) Johnson and (b) Nicolet